Journal of Medicinal Chemistry

Article

Discovery of Novel Spiroindoline Derivatives as Selective Tankyrase Inhibitors

Fumiyuki Shirai, Takeshi Tsumura, Yoko Yashiroda, Hitomi Yuki, Hideaki Niwa, Shin Sato, Tsubasa Chikada, Yasuko Koda, Kenichi Washizuka, Nobuko Yoshimoto, Masako Abe, Tetsuo Onuki, Yui Mazaki, Chizuko Hirama, Takehiro Fukami, Hirofumi Watanabe, Teruki Honma, Takashi Umehara, Mikako Shirouzu, Masayuki Okue, Yuko Kano, Takashi Watanabe, Kouichi Kitamura, Eiki Shitara, Yukiko Muramatsu, Haruka Yoshida, Anna Mizutani, Hiroyuki Seimiya, Minoru Yoshida, and Hiroo Koyama

J. Med. Chem., **Just Accepted Manuscript** • DOI: 10.1021/acs.jmedchem.8b01888 • Publication Date (Web): 18 Mar 2019

Just Accepted

ACS Publications

is published by the American Chemical Society. 1155 Sixteenth Street N.W., Washington, DC 20036

Watanabe, Takashi; Meiji Seika Pharma Co., Ltd., Medicinal Chemistry Laboratory
Kitamura, Kouichi; Meiji Seika Pharma Co., Ltd., Pharmacology Research Laboratory
Shitara, Eiki; Meiji Seika Pharma Co., Ltd., Pharmaceutical Research Division, Pharmaceutical Research Center
Muramatsu, Yukiko; Japanese Foundation for Cancer Research, Division of Molecular Biotherapy, Cancer Chemotherapy Center,
Yoshida, Haruka; Japanese Foundation for Cancer Research, Division of Molecular Biotherapy, Cancer Chemotherapy Center
Mizutani, Anna; Japanese Foundation for Cancer Research, Division of Molecular Biotherapy, Cancer Chemotherapy Center
Seimiya, Hiroyuki; Japanese Foundation for Cancer Research, Division ofMolecular Biotherapy, Cancer Chemotherapy Center
Yoshida, Minoru; RIKEN Center for Sustainable Resource Science, Chemical Genomics Research Group
Koyama, Hiroo; RIKEN Center for Sustainable Resource Science, Drug Discovery Chemistry Platform Unit

Discovery of Novel Spiroindoline Derivatives as Selective Tankyrase Inhibitors

Fumiyuki Shirai[†,*], *Takeshi Tsumura*[§§], *Yoko Yashiroda*[§], *Hitomi Yuki*[††], *Hideaki Niwa*[‡‡], *Shin Sato*[‡‡], *Tsubasa Chikada*[¶¶], *Yasuko Koda*[†], *Kenichi Washizuka*[†], *Nobuko Yoshimoto*[†], *Masako Abe*[‡], *Tetsuo Onuki*[‡], *Yui Mazaki*[§], *Chizuko Hirama*[§], *Takehiro Fukami*[¶], *Hirofumi Watanabe*[††], *Teruki Honma*[††], *Takashi Umehara*[‡‡], *Mikako Shirouzu*[‡‡], *Masayuki Okue*[‡§], *Yuko Kano*[§§], *Takashi Watanabe*[§§], *Kouichi Kitamura*[‡‡], *Eiki Shitara*[†§], *Yukiko Muramatsu*[†¶], *Haruka Yoshida*[†¶], *Anna Mizutani*[†¶], *Hiroyuki Seimiya*[†¶], *Minoru Yoshida*[§, ‡, ‡¶], *Hiroo Koyama*[†,*].

[†]Drug Discovery Chemistry Platform Unit; [‡]Drug Discovery Seed Compounds Exploratory Unit; [§]Chemical Genomics Research Group, RIKEN Center for Sustainable Resource Science; [¶]RIKEN Program for Drug Discovery and Medical Technology Platforms, 2-1 Hirosawa, Wako, Saitama 351-0198, Japan

[††]Drug Discovery Computational Chemistry Platform Unit; [‡‡]Drug Discovery Structural Biology Platform Unit; RIKEN Center for Biosystems Dynamic Research, 1-7-22 Suehiro-cho, Tsurumi-ku, Yokohama, Kanagawa 230-0045, Japan

[§§]Medicinal Chemistry Laboratory; [¶¶]Pharmacokinetics and Analysis Laboratory; [†‡]Pharmacology Research Laboratory; [†§]Pharmaceutical Research Division, Pharmaceutical Research Center; [‡§]Process Chemistry Laboratory, Manufacturing & Control Research Labs, Meiji Seika Pharma Co., Ltd., 760 Morooka-cho, Kohoku-ku, Yokohama, Kanagawa 222-8567, Japan

[†¶]Division of Molecular Biotherapy, Cancer Chemotherapy Center, Japanese Foundation for Cancer Research, 3-8-31 Ariake, Koto-ku, Tokyo 135-8850, Japan

[‡¶]Department of Biotechnology, the University of Tokyo, 1-1-1 Yayoi, Bunkyo-ku, Tokyo 113-8657, Japan

KEYWORDS: tankyrase, Wnt/β-catenin signaling, AXIN, β-catenin, mouse xenograft model, spiroindoline, P-glycoprotein

ABSTRACT: The canonical WNT pathway plays an important role in cancer pathogenesis. Inhibition of poly(ADP-ribose) polymerase catalytic activity of the tankyrases (TNKS/TNKS2) has been reported to reduce the Wnt/β-catenin signal by preventing poly ADP-ribosylation dependent degradation of AXIN, a negative regulator of Wnt/β-catenin signaling. With the goal of investigating the effects of tankyrase and Wnt pathway inhibition on tumor growth, we set out to find small molecule inhibitors of TNKS/TNKS2 with suitable drug-like properties. Starting from **1a**, a high-throughput screening hit, the spiroindoline derivative **40c** (RK-287107) was discovered as a potent TNKS/TNKS2 inhibitor with >7,000-fold selectivity against the PARP1 enzyme, which inhibits WNT-responsive TCF reporter activity and proliferation of human colorectal cancer cell line COLO-320DM. RK-287107 also demonstrated dose-dependent tumor growth inhibition in a mouse xenograft model. These observations suggest that RK-287107 is a promising lead compound for the development of novel tankyrase inhibitors as anticancer agents.

■ INTRODUCTION

The discovery and development of small molecule inhibitors of the canonical WNT pathway, which plays a key role in embryonic development and self-renewal of tissues including the intestinal epithelium,[1] has been a challenging task in cancer drug discovery.[2] Human tumors frequently harbor mutations in genes that encode important proteins such as adenomatous polyposis coli (APC), AXIN, and β-catenin along the WNT pathway.[3] These mutations lead to constitutive activation of WNT signaling, transcription of the genes independent of the WNT ligand stimulation, and aberrant proliferation.[4] It has been reported that a majority (~85%) of colorectal cancers (CRC) carry APC mutations in the WNT signaling pathway.[5] While a number of small molecules have been reported in the literature that can modulate this pathway by targeting various proteins (e.g. Porcupine[6] and β-catenin kinases[7]), no new chemical entity has yet entered the market for the treatment of cancer.[8]

Tankyrases [tankyrase-1: Telomeric repeat binding factor1 (TRF1) interacting ankyrin-related ADP-ribose polymerase-1/ TNKS/ TNKS1/ ARTD5/ PARP-5a; tankyrase-2: TNKS2/ ARTD6/ PARP-5b] constitute a class of the poly(ADP-ribose) polymerase (PARP) enzyme superfamily. All PARP enzymes contain a PARP catalytic domain that can catalyze the post-translational addition of many ADP-riboses successively onto target proteins (PARsylation) using β-NAD^+ as a substrate.[9]

In 2009, a group at Novartis reported that inhibition of the catalytic activity of tankyrases can attenuate the WNT pathway signaling via AXIN stabilization.[10] A small molecule tankyrase inhibitor **XAV939** demonstrated that inhibition of the ubiquitination of AXIN through PARsylation causes accumulation of AXIN. Since AXIN is a concentration-limiting factor in the destruction of the AXIN-β-catenin complex, an increased concentration prevents translocation of

β-catenin to the nucleus and attenuates the transcription of the WNT pathway genes.[11] **XAV939** inhibited colony formation of β-catenin–dependent DLD-1 cells.[10] These findings gave important insights to the therapeutic potential of tankyrase inhibitors for the treatment of cancer.

Because of the highly divergent functions of tankyrases including regulation of the WNT signaling pathway through modification of β-catenin levels, regulation of telomere length[12] and Hippo pathway[13], control of the mitotic checkpoint[14] and vesicle transport modulation[15], the tankyrases have attracted significant interests from pharmaceutical companies as targets of therapeutic intervention.[16] Even though several tankyrase inhibitors in diverse structure classes have been reported and different types of binding motifs have been identified,[17] there have been only a few reports of feasibility studies of tankyrase inhibitors as potential anticancer agents (Fig. 1).

The earliest preclinical study results were reported by Waaler et al. in 2011, where **JW67** and **JW74** were tested in both xenograft and Apc^{Min} mouse models.[18] **JW67** and **JW74** have unique structures as compared with **XAV939** and bind to an induced adenosine pocket[17] of the enzyme. Similar observations have been reported with **JW55**[19] in tamoxifen-induced polyposis formation in conditional Apc truncation mice, where significant reduction of the total tumor area was observed without measurable effects on body weight after 100mg/kg once daily injection for 21 days. In 2013, Lau et al. reported **G007-LK**[20] ,which showed improved antitumor effects with COLO-320DM and SW403 (APC-mutant CRC cell lines) mouse xenograft models.[21] In 2015, a group at Novartis reported **TNKS656**[22], which binds to both nicotinamide and adenosine pockets and exhibited impressive tumor growth suppression in a patient-derived PDX-P30 CRC xenograft model after 100 mg/kg twice daily subcutaneous injection.[23] In 2016, a group at AstraZeneca reported **AZ1366**[24] , which binds only to a nicotinamide subsite and exhibited

significant tumor growth suppression with CRC040 explants after once daily 50mg/kg oral administration for 28 days, where no data on weight loss and/or intestinal toxicity was reported.[25] Since **AZ1366** inhibits PARP1 as well, interpretation of the observed efficacy can be complicated.[26] Importantly, a report from Genentech indicated that a tankyrase inhibitor **G-631**, a nicotinamide pocket binder, caused dose-dependent intestinal toxicity in mice with weak efficacy (100 mg/kg daily oral administration with a SW403 model) and concluded the clinical utility of tankyrase inhibitors by oral administration is likely to be limited because of the "on-target" intestinal toxicity.[27] However, given the availability of structurally diverse tankyrase inhibitors and factors such as tissue distribution variability, we decided to further assess the therapeutic potential of tankyrase inhibitors.[28, 29]

The primary objective of this study was to discover TNKS/TNKS2 dual enzyme inhibitors that disrupt WNT pathway signaling and demonstrate cell growth inhibition of COLO-320DM, which is sensitive to inhibition of Wnt/β-catenin signaling. With the hope of eventually establishing a proof-of-concept that tankyrase inhibitors can suppress tumor growth effectively, we intended to optimize the following characteristics of our compounds: 1) Pharmacokinetic profiles in order to maintain sufficient drug levels during xenograft studies; and 2) PARP selectivity to ensure that the observed efficacy is due to the inhibition of tankyrases, but not of other PARPs, in particular PARP1.[30]

Herein, we describe the discovery of a structurally novel, potent and orally bioavailable TNKS/TNKS2 dual inhibitor, that demonstrated dose-dependent tumor growth inhibition in a mouse COLO-320DM xenograft model when administered orally or intraperitoneally.

■ RESULTS AND DISCUSSION

Identification of HTS hit compound 1a. A high-throughput screening (HTS) of The University of Tokyo Drug Discovery Initiative (DDI) chemical library led to the identification of **1a**, which had IC_{50} values of 20.5 nM and 19.4 nM with the TNKS and TNKS2 enzymes, respectively. Compound **1a** exhibited inhibition of WNT signaling (IC_{50} = 233 nM) in the TCF reporter assay and cell proliferation (GI_{50} = 3.2 μM) in the COLO-320DM CellTiter-Glo luminescence cell viability assay (Fig. 2; Supporting Information Fig. S1).

Table 1 summarizes the *in vitro* activities of **1a**, **XAV939**, and **G007-LK**. As compared with the structurally related **XAV939**, **1a** was less potent than **XAV939** across the enzymes studied. When **1a** was compared with **G007-LK**, belonging to a different structure class, **1a** had more potent enzyme activities and a comparable level of activity in the cellular assays. While the enzyme activities of **1a** were respectable as an HTS hit, low aqueous solubility and mouse liver microsomal stability of **1a** needed to be improved for further development. As encouraged by the relatively small molecular size and potential for structural diversification, and available X-ray co-crystal data, we set out to develop the structure-activity relationship (SAR) of **1a**.

Table 1. Comparison of 1a with XAV939 and G007-LK

Compound	1a	XAV939	G007-LK
TNKS IC_{50} (nM)[a]	20.5	7.5	58.1
TNKS2 IC_{50} (nM)[a]	19.4	3.3	85.5
PARP1 IC_{50} (nM)[a]	>100,000	34,924	>100,000
TCF reporter assay (nM) [a]	233	351	26.7
COLO-320DM GI_{50} (μM)[a] (CellTiter-Glo)	3.2	17.0	1.5
AXIN2 up-regulation@0.33 μM[b]	3.13	4.28	14.34
Aq.Sol. (pH7.4) (μg/mL)	10.0	0.4	1.5
PAMPA ($x10^{-6}$ cm/s)	0.34	3.24	11.4
Hu/Mo PB (% free)[c]	4.3 / 2.9	0.6 / 8.6	2.8 / 3.5
Hu/Mo Mics.Stab. (% remaining@30 min.)[d]	84.1 / 0	78.4 / 0	100 / 95.8

[*a*] Mean values of duplicate or triplicate experiments results. [*b*] Single experiment results. [*c*] Human (Hu) /Mouse (Mo) serum protein binding, % value of free fraction. [*d*] Liver microsomal stability was determined by remaining % of compounds after 30 minutes incubation with human and mouse liver microsome according to the protocol described in the experimental section.

Chemistry

Synthetic modification of compound **1a** was accomplished by the substitution reaction between 2-methylthioquinazolinone analogues (**4a-h**) prepared from ketoesters (**3a-h**) and *o*-, *m*-, or *p*-methoxyphenylpiperazines (*o*-**5**, *m*-**5**, and *p*-**5**) following the published procedure (Scheme 1).[31] Compound **1j** was synthesized by oxidation of **1b**, and **1i** was synthesized by reductive amination of **1h**.

Syntheses of **7-18** are depicted in Scheme 2. Following the same or modified procedure depicted in Scheme 1, compounds (**10-13, 15**, and **16**) were synthesized in one or two steps in moderate to good yields via substitution reactions of 4-(2-methoxyphenyl)piperidine (**19**), or substituted spiropiperidines (**20-22**, **24**, and **25**) with S-oxide of **4a**. Meanwhile, compounds (**7-9**, **14**, **17**, and **18**) were synthesized by a condensation reaction between ethyl 2-cyclohexanonecarboxylate **3a** and corresponding amidine intermediates (e.g. **29**).[32]

Synthesis of substituted spiroindoline/indolinone derivatives was accomplished as outlined in Scheme 3. Following the same procedure for compound **7**, compounds **15a-h** and, **16a-h** were synthesized in two steps; introduction of an amidine functional group and cycloaddition with **3a** to form the tetrahydroquinazolinone (THQ) rings from substituted spiroindoline/indolinone

intermediates (**24** and **25**). For the synthesis of spiroindoline/indolinone derivatives, preparation of the substituted piperidinyl spiro intermediate was the key step. A Fischer indole cyclization reaction was employed between 4-piperidine aldehyde **36** and substituted phenylhydrazines (**37**) to construct a bicyclic spiroindole skeleton [F-I intermediate]. Reduction of the intermediate with sodium triacetoxyborohydride gave the spiroindolines (**38**), while oxidation by *m*-CPBA gave the spiroindolinones (**39**). Benzyloxycarbonyl (Cbz)-deprotection of **38** or **39** with trifluoroacetic acid gave spiro intermediates **24** or **25,** respectively. Boc-protection of **38** or **39**, and deprotection of the Cbz-group under a hydrogenation condition (H_2/ Pd-Carbon) gave spiro intermediates Boc-**24** or Boc-**25**, respectively. Regioisomers with regard to the R-group generated in the Fisher indole synthesis were chromatographically separated at this stage.

Syntheses of analogues with a hydroxyethyl group were accomplished following the approach outlined in Scheme 4. For the indoline series, reductive amination of the THQ-indoline derivatives **15**, **15c**, **15d**, and **15f** with glycolaldehyde dimer and sodium triacetoxyborohydride gave hydroxyethyl substituted compounds **40**, **40c**, **40d**, and **40f**, respectively. For the indolinone series, alkylation of indolinone (**39**) by 2-chloroethyltetrahydropyranyl ether and sodium hydride, and deprotection of the tetrahydropyranyl and Cbz groups under standard conditions, gave 1-hydroxyethyl-indolinone (**42**). Introduction of an amidine group to **42** followed by condensation with keto-ester **3a** gave desired compounds (**43**, **43c**, **43d**, and **43f**). Whereas the synthesis of **42a** and **49a** via Fischer indole cyclization generated regioisomers, we devised a regioselective synthetic route for these compounds (Scheme 4). The spiroindolinone precursor (**42a**) was obtained by *gem*-bis alkylation of commercially available 2-(2,6-difluorophenyl)acetonitrile **44a** with bis(chloroethyl)benzylamine, followed by hydrolysis of the nitrile group to an amide, and a nucleophilic aromatic substitution reaction to spiroindolinone

46a, introduction of 2-hydroxyethyl group to the 1-NH position, and deprotection of the benzyl group. The spiroindoline precursor **49a** was obtained by reduction of spiroindolinone **46a** by lithium aluminum hydride, introduction of a 2-hydroxyethyl group, and deprotection of the benzyl group.

Structure-activity relationship

SAR of tetrahydroquinazolinone analogues. First, we generated a series of tetrahydroquinazolinones with a methoxyphenylpiperidine moiety, which were found to be nicotinamide pocket binders[17] by X-ray crystallography, and tested for their ability to inhibit TNKS/TNKS2 and PARP1 enzyme activities in a biochemical Enzyme-linked immunosorbent assay (ELISA), TCF reporter activity in the human colon cancer DLD-1 cell line for functional activity, and cell proliferation of COLO-320DM cells (Table 2).

Systematic optimization of the 6-position of the bicyclic ring structure revealed that the nicotinamide binding pocket could accommodate methylene, sulfur, oxygen and difluoromethylene moieties in the ring, whereas bulky substituents were not tolerated because enzymatic activity decreases (**1e-j**). We found that a sulfur-containing ring like that of **XAV939** greatly improved the TNKS/TNKS2 enzyme, and cellular TCF reporter activities, but not cell proliferation inhibition activities. This contrast was thought to be due to the vulnerability of the sulfide moiety to oxidation depending on growth period (**1b** vs. **1j**). For potency and aqueous solubility, we decided to preserve the tetrahydroquinazolinone ring (THQ) and shifted our focus to other parts of the molecule.

Analysis of the effects of the substitution pattern of the methoxy group on the phenyl group (*o*-, *m*-, and *p*-methoxy derivatives of **1**) indicated that the ortho substituent gives the most potent enzyme, TCF reporter and cell growth inhibitory activities. It appeared that the ortho-methoxy

group induced a twisted conformation between the piperadine and the phenyl rings because of steric reasons, which was observed in the co-crystal structure (Fig. 3).

Table 2. Modification of tetrahydroquinazoline ring of **1a**

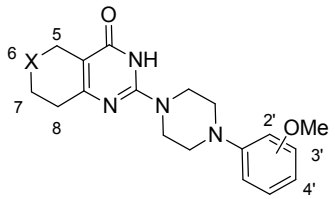

Cmpd	X	Position	TNKS IC_{50} (nM) [a]	TNKS2 IC_{50} (nM) [a]	PARP1 IC_{50} (nM) [b]	TCF Reporter IC_{50} (nM) [a]	COLO-320DM GI_{50} (μM) [c]	Aq.Sol. (pH7.4) (μg/mL)
1 [d]	CH_2	H	135*	58.9*	-	1,536	-	4.9
1a [d]		2'-MeO	20.5	19.4	>20,000	233	3.2	10.0
m-**1a** [e]		3'-MeO	39.4	39.7	>20,000	1,066	14.2	5.2
p-**1a** [e]		4'-MeO	35.0	45.5	>20,000	1,294	>20	4.6
1b	S	2'-MeO	2.5	2.3	>20,000	23.2	3.8	0.5
m-**1b**		3'-MeO	6.2	4.8	>20,000	148	7.4	1.7
p-**1b**		4'-MeO	3.4	2.6	>20,000	114	>50*	0.9
1c	O	2'-MeO	67.6*	112*	>20,000	1,009	17.1	12.3
p-**1c**		4'-MeO	220*	148*	>20,000	2,246	>20*	6.0
1d	CF_2	2'-MeO	19.4	65.5	>20,000	403	15.5*	0.8
p-**1d**		4'-MeO	79.6	36.4	>20,000	1,971	>20*	1.1
1e	$CHCH_3$	2'-MeO	1,350*	3,476*	-	7,282	-	1.8
1f	$C(CH_3)_2$		>20,000*	>20,000*	-	>10,000	-	2.4
1g	CH_2CH_2		5,919*	9,336*	-	>10,000	-	6.9
1h	NH		7,779*	6,984*	-	>10,000	-	66.4
1i	NCH_3		>20,000*	>20,000*	-	>10,000	-	69.7
1j	SO		6,168*	5,345*	>20,000	>10,000	>20*	8.8

[*a*] Mean values are shown from two or three independent experiments carried out in duplicate or triplicate, except that data indicated by asterisks are from a single

experiment carried out in duplicate or triplicate. [*b*] A single experiment was performed in duplicate. [*c*] Three or more independent experiments were performed in triplicate. The asterisk indicates that a single experiment was performed in triplicate. COLO-320DM growth inhibition was evaluated by CellTiter-Glo cell viability assay method. [*d*] Compounds **1** and **1a** were commercially available. [*e*] Tankyrase activities of compounds *m*-**1a**, *p*-**1a** were disclosed in a PCT patent application by Merck GMBH (2013) after evaluation of the compounds. [33]

Interaction of 1a and TNKS2 in a co-crystal structure. In the crystal structure of the **1a** - TNKS2 complex (Fig. 3; Green), the THQ moiety of **1a** binds to the nicotinamide pocket, placing the methoxyphenyl group in the "nook" region.[22] Residues that form the nook region including His1048, Tyr1050, Ile1051, and Gly1053, are TNKS specific and not shared with other PARPs. Thus, close interaction between a ligand and the nook region may contribute to increased PARP selectivity. The carbonyl oxygen of the THQ forms two hydrogen bonds with the hydroxyl group of Ser1068 and the NH group of Gly1032. The nitrogen of the THQ also interacts with the carbonyl group of Gly1032. In addition, the THQ has a π-π interaction with Tyr1071. At the other side of **1a**, the methoxyphenyl group fills the hydrophobic space and forms T-shaped π-π and CH-π interactions with Phe1035 and Ile1075, respectively. The perpendicular orientation of the THQ and terminal benzene rings was thought to be important to

keep the aforementioned close interactions with both the nicotinamide pocket and the nook region. It appeared as though the piperazine moiety connecting the THQ and the terminal phenyl group was simply holding the terminal phenyl ring in a right angle and space without interacting with the enzyme *per se*. (PDB ID: 5ZQO; Supporting Information Table S10)

SAR of the right-hand substructure. Structural modification of the connecting piece between the THQ and the phenyl ring was conducted with the intention of placing the phenyl group perpendicular to the connecting ring structure (Table 3).

Table 3. Optimization of the connecting structure to improve potency and solubility

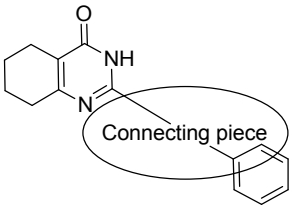

Cmpd	Connecting piece - Ar	Y	TNKS IC_{50} (nM)[a]	TNKS2 IC_{50} (nM)[a]	PARP1 IC_{50} (nM)[b]	TCF Reporter IC_{50} (nM)[a]	COLO-320DM GI_{50} (μM)[a]	Aq.Sol. (pH7.4) (μg/mL)	Hu/Mo Mic.Stab. (%) @30min
1a	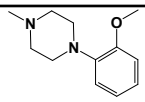	-	20.5	19.4	>20,000	233	3.2	10.0	84.1/0.0
7	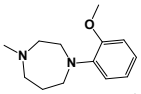	-	6,008*	4,386*	>20,000	9,144	41.9*	69.6	-
8	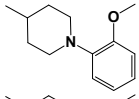	-	14,300*	6,417*	-	5,401	19.6*	-	-
9	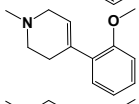	-	35.0	49.7	>20,000	1,161	6.3	14.2	99.3/91.7
10[c]	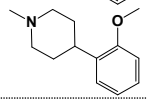	-	65.4	67.6	>20,000	531	4.6	1.0	62.1/0.0
11	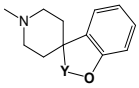	CH_2	43.4	14.6	>20,000	608	10.8	0.67	64.3/0.1
12		C=O	30.2	18.3	>20,000	>10,000	>50	1.17	28.1/0.1
13	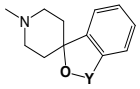	CH_2	31.5	35.7	>20,000	342	5.8	1.07	76.3/0.0
14		C=O	33.7	21.0	>20,000	1,347	26.9	31.6	34.3/0.3
15	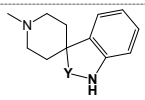	CH_2	28.5	20.7	>20,000	352	13.1	1.6	77.9/34.7
16		C=O	27.6	25.1	>20,000	591	11.2	64.2	84.3/0.0
17	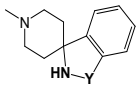	CH_2	118*	29.3*	>20,000	1,605	22.4*	67.0	-
18		C=O	514*	258*	>20,000	>10,000	97.7*	70.1	-

[*a*] Mean values are shown from two or more independent experiments performed in duplicate or triplicate. The asterisk indicates that a single experiment was performed in duplicate or triplicate. [*b*] A single experiment was performed in duplicate. [*c*] Tankyrase

activities of compound **10** were disclosed in a PCT patent application by Merck GMBH (2013) after evaluation of the compound had been completed.[33]

Comparison of the activities of **7** and **8** with **1a** suggested that the enzyme activities are sensitive to the placement of the terminal phenyl ring. Compound **9**, which replaces the piperazine moiety of **1a** with a 1,2,3,6-tetrahydropyridine, showed comparable enzyme and cellular functional activity with **1a**. Compound **10**[33], which replaces the piperazine moiety of **1a** with a piperidine moiety, also showed enzyme and cellular functional activities comparable to **1a**. These observations prompted us to investigate a new series of compounds that would hold the terminal phenyl ring perpendicular to the connecting ring structure, namely compounds with bicyclic spiro structures (**11-18**).(Fig. 2)

Analogues comparable in enzymatic potencies to **1a** include benzofuran derivatives (**11** and **12**), whose structures could be viewed as the products of connecting the methoxy group of the terminal phenyl group and the piperidine C-4 carbon of **10** (Fig. 2), isobenzofurane (**13** and **14**) and indoline derivatives (**15** and **16**) (TNKS/TNKS2 IC_{50} = 15 - 45 nM) although cellular activities were somewhat diminished. While none of the newly synthesized compounds showed superior in vitro profiles both in liver microsomal stability and aqueous solubility as compared with **1a**, spiroindoline compound **15** and spiroindolinone compound **16** showed superior microsomal stability, and significantly higher aqueous solubility, respectively. Based on these findings, we decided to continue with the SAR development of the spiroindoline and spiroindolinone series.

SAR of substituted spiro indoline/indolinone derivatives to improve *in vitro* activities. Then we shifted our focus to the substituents at the 4- and/or 6-position of the phenyl ring for improved enzyme activity. (Table 4)

Introduction of halogen atoms, such as F and Cl to the 4- and 4, 6-positions of **15** and **16** resulted in improved enzyme, cellular TCF reporter and cell growth inhibitory activities (**15a**, **c**, and **d**; **16a**, **c**, and **d**), while other substitution patterns on the phenyl ring (e.g. ethers, amines, and amides) were not fruitful (data not shown). Low aqueous solubility of these derivatives discouraged us from further investigation.

In an attempt to explain the improved activities of the halogen-substituted indoline series, we applied the fragment molecular orbital (FMO) method[34, 35, 36] for compounds **15** and, **15a-d**. Pair interaction energy decomposition analysis based on FMO calculations showed high correlation between TNKS2 enzyme IC_{50} values and the interaction energies of two fragments, Tyr1050 and Pro1034. A hydrogen bond was observed between the hydrogen attached to the nitrogen of indoline and the main-chain carbonyl oxygen of Ala1049 (assigned to the Tyr1050 fragment, see computational methods section for details) in the X-ray structure of TNKS2 and **15d** (PDB ID: 6A84; Supporting Information Fig. S9; Table S10). Introduction of halogen(s) causes a small increase of the positive charge of the indoline hydrogen, which enhances the hydrogen-bonding interaction. In addition, introduction of halogen(s) to the indoline, especially at the 4-position, causes a charge transfer interaction between the phenyl ring and Pro1034. These two interactions with the main-chain carbonyl oxygen of Ala1049 and Pro1034 are thought to be responsible for the improved enzyme activities (Supporting Information Fig. S2; Table S5 and S6).

Table 4. Optimization of the substituents of the spiroindoline/indolinone derivatives for enzyme and cellular activities

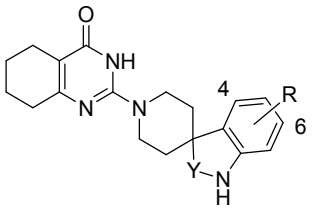

Compound	Y	R	TNKS IC_{50} (nM)[a]	TNKS2 IC_{50} (nM)[a]	TCF Reporter IC_{50}(nM)[a]	COLO-320DM GI_{50} (μM)[a]	Aq.Sol. (pH7.4) (μg/mL)
15	CH_2	H	28.5	20.7	352	13.1	1.6
15a		4-F	4.4	2.8	72.4	3.3	4.2
15b		6-F	16.7	7.6	657	10.3	3.2
15c		4,6-diF	5.4	3.3	110	5.2	6.3
15d		4-Cl	6.4	5.3	247	4.9	2.6
15e		6-Cl	8.4	5.8	818	6.9	9.2
15f		4,6-diCl	7.5	10.4	609	7.5	11.0
15g		4-Br	16.0	15.6	454	10.4	8.9
15h		4-CN	9.9*	18.5*	799	23.6*	69.2
16	C=O	H	27.6	25.1	591	11.2	64.2
16a		4-F	5.8	4.7	31.1	2.3	3.1
16b		6-F	11.0	12.0	369	15.0	62.9
16c		4,6-diF	6.4	7.5	43.9	4.2	0.8
16d		4-Cl	10.2	4.9	21.5	5.0	2.8
16e		6-Cl	11.1	14.4	623	19.9	1.8
16f		4,6-diCl	5.3	7.1	533	21.4	15.7
16g		4-Br	5.8	13.4	91.2	8.8	1.9
16h		4-CN	16.8*	26.8*	496	20.4*	5.3

[*a*] Mean values are shown from two or more independent experiments performed in duplicate or triplicate. The asterisk indicates that a single experiment was performed in duplicate or triplicate.

Table 5. SAR of hydroxyethyl substituted spiroindoline/indolinone derivatives to improve aqueous solubility

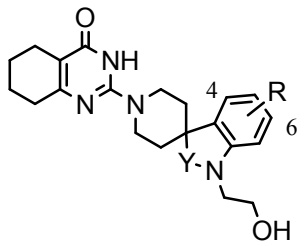

Cmpd	Y	R	TNKS IC_{50} (nM)[a]	TNKS2 IC_{50} (nM)[a]	PARP-1 IC_{50} (nM)[b]	TCF Reporter IC_{50} (nM)[a]	COLO-320DM GI_{50} (μM)[c]	COLO-320DM (MTT) GI_{50} (μM)[c]	RKO (MTT) GI_{50} (μM)[c]	AXIN2 up-regulation @0.1μM	Aq.Sol. (pH7.4, μg/mL)[e]	PAMPA ($x10^{-6}$ cm/s)
40	CH_2	H	49.3	26.9	>20,000	362	3.9	1.77	0.22	0.98	>76.1	17.4
40a		4-F	9.2	11.8	>20,000	83.9	1.4	0.26	0.09	3.63	74.6	7.6
40d		4-Cl	16.6	17.0	>20,000	52.9	1.5	0.30	>10[d]	4.86	2.5*	-
40c		4,6-diF	14.3	10.6	>20,000	77.6	1.6	0.45[f]	>10[d, f]	4.42	72.1	2.0
40f		4,6-diCl	18.2	16.4	>20,000	119	2.9	4.65	0.04	4.03	5.2*	-
43	C=O	H	19.0	26.0	>20,000	918	12.7	2.67	3.40	0.98	78.7	2.9
43a		4-F	6.8	8.2	>20,000	36.5	1.8	0.19	2.03	4.10	80.1	3.6
43d		4-Cl	4.4	6.8	>20,000	13.9	1.0	0.25	>10[d]	5.75	84.5	1.1
43c		4,6-diF	10.0	15.1	>20,000	79.4	2.4	0.47	>10[d]	3.93	76.9	7.9
43f		4,6-diCl	9.0	9.5	>20,000	19.8	2.6	0.45	2.61	8.03	55.9	43.0

[*a*] Mean values are shown from two or more independent experiments performed in duplicate or triplicate. [*b*] A single experiment was performed in duplicate. [*c*] Mean values are shown from three or more independent experiments performed in triplicate. [*d*] While the cell number was marginally reduced at 0.3 μM of the compound to the

maximal extent, the relative cell numbers were maintained higher than 50% of untreated cells at any doses examined (see Figure S4). [*e*] In general, single experiment has been performed. The asterisk indicates two experiments have been performed. [*f*] Data were disclosed in ref. 41.

Introduction of the hydroxyethyl substituent to improve drug-like properties. For improved aqueous solubility, we decided to introduce a hydroxyethyl group to the 1-NH position of the indoline/indolinone series (Table 5). Introduction of a hydroxyethyl moiety to halogen substituted derivatives was tolerated in enzyme (IC_{50} = 4 - 18 nM) and TCF reporter (14 - 120 nM) inhibitory activities, and cell proliferation inhibition (GI_{50}= 1.0 - 2.9 μM) while contributing to improved aqueous solubility (**40a**, **40c**, **43a**, **43c**, **43d**, and **43f**). Meanwhile, compounds (**40a**, **40f**, **43a** and **43f**) exhibited moderate to potent growth inhibition of both COLO-320DM and RKO cells, presumably due to unspecified off-target effects. Compounds **40c**, **40d**, **43c**, and **43d** were selected for further evaluations (Supporting Information Fig. S4).

Crystal structure of spiro compounds with TNKS2. According to the crystal structure of compound **12** (Fig. 4; magenta), the THQ moiety forms the same hydrogen bonds and π–π interactions as **1a** (Fig. 4; green) in the nicotinamide pocket. The spirobenzofuranone of **12** also fits in the hydrophobic pocket and makes π-stacking interactions with Phe1035 and interacts with Ile1075, just like the methoxyphenyl group of **1a** (PDB ID: 5ZQP). As compared with the rotating methoxyphenyl group of **1a**, the structurally rigid spirobenzofuranone of **12** may contribute to binding affinity more effectively. Since **1a** and **12** share the same spiropiperidine ring, placement of the spirobenzofuranone group is nearly superimposable, but the phenyl rings were in opposite orientations. The inversion of the benzofuranone ring seems to be set by the π-π

interaction with Phe1035, CH-π interaction with Ile1075, and long-range weak interaction between the oxygen in the furan moiety and the nitrogen of Ile1075 via a water molecule. In contrast, X-ray crystallography of **52**, an N-methyl derivative of **16**, indicated that the indole phenyl ring was overlapping with the phenyl ring of **1a** as a result of the π–π interaction with both Phe1035 and Ile1075 (PDB ID: 5ZQQ; Supporting Information Fig. S10, Table S10).

In the co-crystal structure of **40c** with TNKS2 (Fig.5; blue), **40c** fits in the nicotinamide binding pocket with the indole phenyl ring overlapping the phenyl ring of **1a** and **52**. The hydroxyethyl group on the nitrogen of the spiroindoline **40c** forms a hydrogen bond with the OH group of Ser1033 via a water molecule (PDB ID: 5ZQR; Supporting Information Table S10).

Pharmacokinetic profiles. To assess the potential for *in vivo* efficacy, we studied serum protein binding, liver microsomal stability, and P-glycoprotein (P-gp/MDR1) mediated efflux ratio using a method of cell systems which involve MDR1 overexpressing MDCKII cells.[37]

In the serum protein binding studies, free fractions of the indolinones (**43c** and **43d**) were higher than that of indolines (**40c** and **40d**). By the introduction of the hydroxyethyl group, mouse liver microsomal stability of the indolinones improved as compared with the indolines. As compared with the indolines, the indolinones exhibited significantly higher aqueous solubility, lower human serum protein binding, and better liver microsomal stability, whereas the efflux ratios of both MDR1-overexpressed and normal MDCK cells were higher with the indolinones than the indolines. Increased efflux ratios of 1-hydroxyethylindolinones may be attributed to the additional substituent change of the indolinone with a lone pair of the carbonyl moiety (Table 6).

P-glycoprotein is a clinically important transmembrane transporter in chemotherapy due to its wide-ranging effects on the absorption and excretion of drugs, and it therefore confers a multi-

drug resistance phenotype to cancer cells.[38] Based on a report of a drug resistant tumor xenograft model using a P-gp inhibitor, we assumed that the P-gp efflux ratio is an important factor when selecting compounds for *in vivo* efficacy studies.[39]

Table 6. Biochemical properties and pharmacokinetic profiles of selected compounds

THQ= 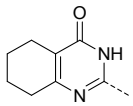

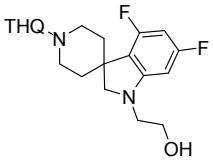

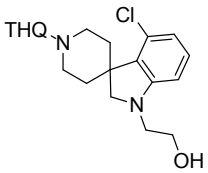

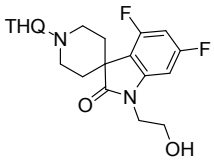

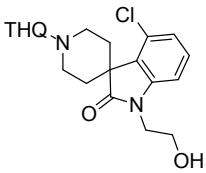

Compound	40c	40d	43c	43d
Hu/Mo PB[a](% free)	0.4 / 1.5	0.9 / 1.0	1.7 / 7.7	1.8 / 4.2
Hu/Mo Mics.Stab. (%) remaining@30min	5.9 / 18.3	6.1 / 1.1	39.5 / 39.1	28.9 / 19.1
MDCK efflux ratio	1.8	1.7	3.3	3.7
MDCK-MDR1 efflux ratio	5.3	5.1	16.1	18.8
Mouse IP[b] C_{max} (μmol/L)	199.2	75.6	48.1	53.5
$t_{1/2}$ (h)	2.8	4.8	3.6	4.1
AUC_{inf} (μmol/L*h)	555	667	106	157

[*a*] Hu/Mo PB: Human/Mouse serum protein binding, % value of free fraction. [*b*] Mouse intraperitoneal (IP) injection, Dose 50mg/kg, ICR mouse.

Pharmacokinetic studies (mouse intraperitoneal injection) indicated that the maximum concentration (C_{max}) of **40c** was four times higher than that of **43c** and **43d**, and that the exposure levels (compared with the area under the curve [AUC_{inf}]) of **40c** and **40d** were about four times higher than that of **43c** and **43d**. Lower C_{max} of **40d** was thought to be due to low aqueous solubility. These results may be derived from the intestinal and renal efflux, rather than differences in lipophilicity, given that the differences in membrane permeability were relatively small and the value of **40c** was rather lower when **40c** and **43c** were compared (2.0 and 7.9 x10^{-6} cm/s, respectively; Table 5).

Moreover, as for the mouse pharmacokinetics of **40c**, the exposure level (AUC_{inf}) when orally administered at the 50mg/kg dose was about a half of that of the intraperitoneal administration (Supporting Information Fig. S7), and the bioavailability (F value) for rat pharmacokinetics was 59.8% (Table 7, Supporting Information Fig. S8). Compound **40c** was well absorbed from the gastrointestinal tract resulting in high plasma drug levels. Overall, **40c** appeared to have the most desirable mouse pharmacokinetic properties for *in vivo* experiments, albeit with slightly lower liver microsomal stability.

Profile of tankyrase inhibitor 40c. To assess the biological target specificity of **40c**, inhibition of human PARP family member enzymes PARP1, PARP2 (poly ADP-ribosylation) and PARP10 (mono ADP-ribosylation) was tested.[40] None of the tested PARP enzymes were strongly inhibited by **40c,** comparing inhibitory activity of PARP1 (>100,000 nM), PARP2 (2,717 nM) and PARP10 (19,807 nM) with the activity of TNKS and TNKS2 (14.3 nM and 10.6 nM, respectively) (Table 7; Supporting Information Fig. S5). Furthermore, **40c** was evaluated on the screen panel of forty-four kinds of protein kinases, phosphatases, ion channels, GPCRs and transporters at 10 μM concentration (SafetyScreen44, Eurofins), and no hit protein with over 20% inhibition was observed. (Supporting Information Table S7)

Quantitative RT-PCR assay of **40c** with the benchmark compound G007-LK to specify the target genes of β-catenin and hippo pathway was evaluated. After treatment of COLO-320DM cells with the inhibitors for 48 h, relative expression levels of AXIN2, TCF7, AMOTL2, CTGF and CYR61 transcripts were determined by normalization with those of ACTB expression.[41] It revealed that down-regulation of AXIN2 and TCF7 transcripts by β-catenin pathway were inevitably observed, but obvious changes of AMOTL2, CTGF and CYR61 transcripts by hippo pathway was not observed in COLO-320DM cells. (Supporting Information Fig. S6)

Compound **40c** has been reported to demonstrate efficacy in mouse COLO-320DM xenograft models with intraperitoneal and oral administration.[42] Upon 150 mg/kg twice daily (BID) intraperitoneal administration to mice (n = 9) bearing human COLO-320DM tumors for 11 days, **40c** exhibited statistically significant tumor growth inhibition (TGI = 47.2%, $p < 0.01$) without notable weight loss or toxicity. In contrast, **G007-LK** was reported to inhibit tumor growth (48% TGI) at 40 mg/kg daily intraperitoneal administration together with detectable weight loss.[21] Meanwhile, **40c** exhibited statically significant tumor growth inhibition (TGI = 51.9%, $p < 0.05$) with slightly lower body weight when administered orally at 300 mg/kg, BID to the model mouse (n = 9). Recently, Anumala et al. also reported no animal discomforts or body weight differences in xenograft model with their tankyrase inhibitor.[43]

■ CONCLUSION

Multifactorial optimization of a HTS hit compound **1a**, led to the identification of a spiroindoline derivative **40c** (RK-287107). RK-287107 is a potent TNKS/TNKS2 inhibitor with high selectivity against other PARP family members, PARP1 (IC_{50} = >100,000 nM: >7,000-fold), PARP2 (IC_{50} = 2,717 nM: ~200-fold) and PARP10 (IC_{50} = 19,807 nM: >1,000-fold). At the cellular level, RK-287107 inhibits the Wnt/β-catenin signaling pathway as indicated by a TCF reporter assay in DLD-1 and HEK293 cells (IC_{50} = 77.6 nM and 83.0 nM, respectively), and also inhibits the proliferation of human colorectal cancer COLO-320DM cells to the same extent as **G007-LK** (Table 7). Analysis of correlation between pIC_{50} value of TNKS/TNKS2 enzymes and that of TCF reporter assay in DLD-1 cells revealed that the enzyme inhibitory activities are significantly correlated with the functional inhibition of Wnt/β-catenin signaling with Pearson correlation coefficients (r = 0.767 / 0.747), respectively. RK-287107 modulates β-catenin pathway by down-regulation of AXIN2 and TCF7 transcripts as revealed by quantitative RT-

PCR assay in COLO-320DM cells. RK-287107 exhibited very weak or no activities with forty-four kinds of important safety-related proteins. Furthermore, RK-287107 showed impressive pharmacokinetic profiles with rat bioavailability of approximately 60%.

In a COLO-320DM xenograft model, RK-0287107 exhibited moderate tumor growth inhibition at a relatively high dose, presumably because of insufficient cellular activity and drug duration by low microsomal stability. It was noteworthy that weight loss and general toxicity was not observed at doses where statistically significant efficacy was observed. These results suggest that RK-287107 is an attractive lead compound for the development of new tankyrase inhibitors and provide valuable insights into the potential utility of tankyrase inhibitors for the treatment of various forms of cancer.

Table 7. *In vitro* and rat pharmacokinetic properties of RK-287107 (**40c**) in comparison to **1a** and **G007-LK**

Compound	RK-287107 (40c)	1a	G007-LK
TNKS enz IC_{50} (nM)	**14.3**	20.5	58.1
TNKS2 enz IC_{50} (nM)	**10.6**	19.4	85.5
PARP1 enz IC_{50} (nM)	>100,000	>100,000	>100,000
PARP2 enz IC_{50} (nM)	2,717	2,230	>100,000
PARP10 enz IC_{50} (nM)	19,807	10,155	>100,000
TCF reporter DLD-1 / HEK293 IC_{50} (nM)	**77.6 / 12.1**	233 / 42.9	26.7 / 4.5
Colo-320DM (CellTiter-Glo) GI_{50} (μM)	**1.6**	3.2	1.5
Colo-320DM (MTT) GI_{50} (μM)	**0.45**[a]	1.82[a]	0.43[a]
RKO (MTT) GI_{50} (μM)	**>10**	-	8.90
AXIN2 up-regulation@0.1 μM	4.42	3.13[b]	5.84
Aq.Sol. (pH7.4) (μg/mL)	**72.1**	10.0	1.5
PAMPA ($x10^{-6}$ cm/s)	**2.0**	0.34	11.4
Hu/Mo PB (% free)	0.4 / 1.5	4.3 / 2.9	2.8 / 3.5
Hu/Mo Mics.Stab. (%) remaining@30min.	5.9 / 18.3	84.1 / 0.0	100 / 95.8
MDCKII / MDCKII-MDR1 Flux ratio (AtoB vs BtoA)	1.8 / 5.3	1.0 / 1.0	1.0 / 3.5
Rat IV[c] C_0 (μmol/L)	**9.84**	1.00	1.54
$T_{1/2}$ (hr)	3.5	13.0	3.3
AUC_{inf} (μmol/L*hr)	**4.42**	0.72	0.79
CL_{tot} (L/hr/kg)	**0.54**	4.08	2.38
Vdss (L/kg)	0.59	58.9	1.79
Rat PO[d] C_{max} (μmol/L)	**2.28**	0.12	0.23
T_{max} (hr)	0.25	0.5	4.0
AUC_{inf} (μmol/L*hr)	**7.92**	1.27	2.33
F (%)	59.8	59.7	97.8

Bold characters mean improved properties on **1a**. [*a*] Data are from ref. 41. [*b*] AXIN2 up-regulation at 0.33 μM. [*c*] Rat intravenous (IV) injection at 1 mg/kg. [*d*] Rat per oral (PO) injection at 3 mg/kg, Sprague-Dawley rat.

■ EXPERIMENTAL SECTION

High-throughput screening

To identify tankyrase inhibitors, HTS of compounds provided by DDI was conducted by using the yeast cell-based method as previously reported[44]. Briefly, preculture of the tankyrase-1 overexpression fission yeast (*Schizosaccharomyces pombe*) strain was 200-fold diluted in minimal medium (MM) that induced the TNKS gene expression and was grown in 20 μL of MM media containing each tested compound at a concentration of 20 μM using 384-well plates at 30 °C for 18-22 h. Yeast cell growth was assessed using WST-1 reagent that measured mitochondrial dehydrogenase activity. Since overexpression of the TNKS gene caused growth defects to the yeast, compounds that recovered the growth defect were identified as potential tankyrase inhibitors. As shown in Fig. S1, among 141,117 compounds provided by DDI, we selected 640 compounds that showed over 17% recovery; "17% recovery" was shown in the presence of flavone that was identified and validated as a tankyrase inhibitor[44]. Then, we carried out an enzyme-linked immunosorbent assay (ELISA) for TNKS as described below and selected 58 compounds that showed over 50% inhibitory activity at 20 μM. Out of 58 compounds, 44 compounds were commercially available and were evaluated by calculating IC_{50} values for TNKS, TNKS2, and PARP1 using ELISA. (Supporting Information Figure S1)

Chemistry

General procedure. All chemicals were purchased from commercial suppliers TCI, Wako, and Sigma-Aldrich, and used as received unless otherwise specified. NMR spectra were recorded at either 270 MHz (JEOL JNM-Ex270), 400 MHz (JEOL ECS-400 or Bruker 400MHz Advance III HD) spectrometers. Chemical shifts are reported in ppm (δ) referenced to TMS (δ = 0.00 ppm), DMSO (2.50 ppm), and $CHCl_3$ (7.26 ppm). Temperatures are expressed in degrees Celsius (°C)

and are uncorrected. Purity and characterization of all final compounds were established by a combination of LC−MS and NMR analytical techniques. Final compounds were found to be >95% pure by HPLC analysis (λ = 254nm). LC−MS analysis was performed on a Waters Acquity UPLC analytical system with DAD coupled to a single quadrupole mass spectrometer (ESI-SQ) equipped with an ACQUITY UPLC BEH C18 column, 2.1 mm × 50 mm, 1.7 µm. Method: ESI+, flux of 0.6 mL/min, 5−95% CH_3CN in H_2O + 0.1% TFA, total run time of 2 min. High-resolution mass spectrometry (HRMS) analysis was performed using hybrid quadrupole/time-of-flight tandem mass spectrometer, Synapt G2 instrument (Waters) for final compounds. Microwave reaction was carried using Initiator 2.5, Biotage Japan.

Materials. XAV939 was purchased from Tocris bioscience, UK. **G007-LK** was synthesized by a partially modified method reported in the literature[20]. CAS numbers of reported compound are listed. (**1**: 33017-98-0; **1a**: 925643-44-3; *m*-**1a**: 924864-18-6; *p*-**1a**: 878433-57-9: **10**: 1449693-53-1)

2-(4-(2-Methoxyphenyl)piperazin-1-yl)-3,5,7,8-tetrahydro-4*H*-thiopyrano[4,3-d]pyrimidin-4-one (1b). Compound **4b** (1 equiv, 500 mg, 2.33 mmol) and 1-(2-methoxyphenyl)piperazine (1.2 equiv, 538 mg, 2.80 mmol) were suspended in toluene (50 mL), and the mixture was stirred under reflux condition for 4 days. The reaction mixture was evaporated under reduced pressure and the residue was column chromatographed on silica gel and amino silica gel (chloroform/methanol = 100:0–90:10) and desired fractions were evaporated to give 288 mg (34%, 0.80 mmol) of compound **1b** as a white solid; LC-MS (ESI) m/z 359 ($M + H^+$). Retention time: 1.06 min. LC Purity: 97.5%. HRMS m/z ($M + H^+$) observed for $C_{18}H_{22}N_4O_2S + H^+$: 359.1542, found: 359.1534. ^1H NMR (270 MHz, $CDCl_3$) δ [ppm] 2.77-2.91 (m, 4H), 3.13 (t, *J*= 4.95 Hz, 4H), 3.51-3.58 (m, 2H), 3.83-3.94 (m, 4H), 3.91 (s, 3H), 6.86-7.00 (m, 3H), 7.00-7.10

(m, 1H), 11.81 (br s, 1H). Compounds **1a**, **m-1b, p-1b**, **1c**, **1d**, **1e**, **1f**, and **1g** were prepared from the corresponding intermediates (**4**) following the same procedure as compound **1b**. ^{1}H NMR spectra, MS and other experimental data are provided in Supporting Information.

2-(4-(2-Methoxyphenyl)piperazin-1-yl)-5,6,7,8-tetrahydropyrido[4,3-*d*]pyrimidin-4(3*H*)-one (1h). Compound **4h** (1 equiv, 319 mg, 1.07 mmol) and 1-(2-methoxyphenyl)piperazine (1.2 equiv, 248 mg, 1.29 mmol) was suspended in toluene (30 mL) and the mixture was stirred under reflux condition for 3 days. The reaction mixture was evaporated under reduced pressure and column chromatographed on amino silica gel and silica gel (chloroform/methanol = 100:0-90:10) and desired fractions were evaporated to give 301.8 mg (64%, 0.68 mmol) of compound Boc-**1h** as a solid; LC-MS (ESI) m/z 442 (M + H$^+$) observed for $C_{23}H_{31}N_5O_4$ + H$^+$. Retention time: 1.21 min. LC Purity: 92.7%. ^{1}H NMR (270 MHz, $CDCl_3$) δ [ppm] 1.45 (br s, 1H), 1.57 (s, 9H), 2.55-2.61 (m, 2H), 3.11-3.17 (m, 2H), 3.60-3.66 (m, 4H), 3.82-3.88 (m, 4H), 3.90 (s, 3H), 4.23-4.27 (m, 2H), 6.85-7.12 (m, 4H),

4N hydrogen chloride in dioxane (9.7 equiv, 1.4 ml, 5.60 mmol) was added to compound Boc-**1h** (254 mg, 0.58 mmol) and the mixture was stirred for 4 hours and evaporated under reduced pressure. The residue was triturated with diisopropyl ether to give 122 mg (62%, 0.36 mmol) of compound **1h** as a white solid; LC-MS (ESI) m/z 342 (M + H$^+$). Retention time: 0.88 min. LC Purity: 97.5%. HRMS m/z (M + H$^+$) calculated for $C_{18}H_{23}N_5O_2$ + H$^+$: 342.1930, found: 342.1931. ^{1}H NMR (270 MHz, $CDCl_3$) δ [ppm] 2.50-2.59 (m, 2H), 2.99-3.17 (m, 4H), 3.37 (br d, *J*= 1.65 Hz, 4H), 3.68 (s, 2H), 3.87-3.93 (m, 4H), 3.95 (s, 3H), 6.86-7.12 (m, 4H).

2-(4-(2-Methoxyphenyl)piperazin-1-yl)-6-methyl-5,6,7,8-tetrahydropyrido[4,3-*d*]pyrimidin-4(3*H*)-one (1i). To a solution of compound **1h** (1 equiv, 103.7 mg, 0.30 mmol) in methanol (4 mL) was added 37% (w/w) formaldehyde (7.3 equiv, 180 µL, 2.22 mmol), acetic acid (2 equiv,

54 μL, 0.60 mmol), and sodium cyanoborohydride (2.5 equiv, 48 mg, 0.75 mmol) at ambient temperature. The reaction mixture was stirred for 1 hour, and then diluted with chloroform, 1N aqueous sodium hydroxide and saturated sodium chloride. The mixture was extracted four times with chloroform, washed with saturated sodium chloride, dried over sodium sulfate, filtered and evaporated under reduced pressure. The residue was column chromatographed on amino silica gel and desired fractions were evaporated to give 79.6 mg (73%, 0.22 mmol) of compound **1i** as a white solid; LC-MS (ESI) m/z 356 (M + H^+). Retention time: 0.85 min. LC Purity: >99%. HRMS m/z (M + H^+) calculated for $C_{19}H_{25}N_5O_2$ + H^+: 356.2086, found: 356.2083. ^{1}H NMR (270 MHz, $CDCl_3$) δ [ppm] 1.60 (br s, 1H), 2.46 (s, 3H), 2.66 (s, 4H), 3.13 (br t, *J*= 5.93 Hz, 4H), 3.31 (s, 2H), 3.83 (br t, *J*= 5.28 Hz, 4H), 3.90 (s, 3H), 6.87-7.09 (m, 4H).

2-(4-(2-Methoxyphenyl)piperazin-1-yl)-3,5,7,8-tetrahydro-4H-thiopyrano[4,3-d]pyrimidin-4-one 6-oxide (1j). To a solution of compound **1b** (1 equiv, 150 mg, 0.42 mmol) in dichloromethane (15 mL) was added m-chloroperbenzoic acid (1.2 equiv, 116 mg, 0.50 mmol) at ambient temperature and stirred 1 hour. The reaction mixture was washed with saturated sodium hydrogen carbonate, water and saturated sodium chloride, dried over sodium sulfate, filtered and evaporated under reduced pressure. The residue was column chromatographed on amino silica gel and desired fractions were evaporated to give 114 mg (70%, 0.29 mmol) of compound **1j** as a white solid; LC-MS (ESI) m/z 375 (M + H^+). Retention time: 1.08min. LC Purity: >99%. HRMS m/z (M + H^+) calculated for $C_{18}H_{22}N_4O_3S$ + H^+: 375.1491, found: 375.1485. ^{1}H NMR (270 MHz, $CDCl_3$) δ [ppm] 2.74-2.97 (m, 2H), 3.08-3.30 (m, 6H), 3.64-3.84 (m, 2H), 3.86-3.97 (m, 7H), 6.89-6.99 (m, 3H), 7.02-7.11 (m, 1H), 11.86 (br s, 1H).

2-(Methylthio)-3,5,7,8-tetrahydro-4*H*-thiopyrano[4,3-d]pyrimidin-4-one (4b). To a suspension of ethyl 4-oxotetrahydro-2*H*-thiopyran-3-carboxylate (**3b**, 2.0 g, 10.6 mmol) in water

(20 mL) was added S-methylisothiourea sulfate (1.14 equiv, 3.35 g, 12.3 mmol) and potassium carbonate (2.2 equiv, 3.23 g, 23.4 mmol) at ambient temperature. The reaction mixture was stirred for 20 hours. The precipitate was collected, washed with water (twice) and isopropyl ether, and dried to give 2.28 g (quant., 10.6 mmol) of compound **4b** as a white solid; LC-MS (ESI) m/z 215 (M + H^+) observed for $C_8H_{10}N_2OS_2$ + H^+. Retention time: 1.06 min. ^{1}H NMR (270 MHz, $CDCl_3$): δ [ppm] 2.54 (s, 3H), 2.81-2.97 (m, 4H), 3.59 (s, 2H), 5.10 (br s, 1H).

Compounds **4a** and **4g** were prepared from the corresponding keto-esters (**3**) following the same procedure as compound **4b**.

6,6-Difluoro-2-(methylthio)-5,6,7,8-tetrahydroquinazolin-4(3*H*)-one (4d). To a solution of diethyl 4, 4-difluoroheptanedioate (**6**, 1 equiv, 1.0 g, 3.96 mmol) in toluene was added potassium t-butoxide (1.5 equiv, 0.67 g, 5.97 mmol) at ambient temperature. After stirring overnight, the reaction mixture was quenched with 1N aqueous hydrochloric acid and extracted with ethyl acetate. The organic layer was washed twice with water, dried over magnesium sulfate, and evaporated under reduced pressure to give 792 mg (97%, 3.83 mmol) of crude ethyl 5,5-difluoro-2-cyclohexanonecarboxylate **3d** as oil. To a suspension of crude compound **3d** (1 equiv, 780 mg, 3.77 mmol) in water (8 mL) was added S-methylisothiourea sulfate (1.27 equiv, 1.3 g, 4.78 mmol) and potassium carbonate (2.4 equiv, 1.25 g, 9.04 mmol) at ambient temperature. The reaction mixture was stirred at 50 °C. After stirring overnight, the reaction mixture was quenched with 1N aqueous hydrochloric acid and extracted with ethyl acetate. The organic layer was washed with water and saturated sodium chloride, dried over magnesium sulfate, evaporated under reduced pressure, triturated with isopropyl ether and filtered. The residue was washed with isopropyl ether and dried to give 633 mg (72%, 2.71 mmol) of compound **4d** as a white solid; LC-MS (ESI) m/z 233 (M + H^+) observed for $C_9H_{10}F_2N_2OS$ + H^+. Retention time: 1.15 min. ^{1}H

NMR (270 MHz, $CDCl_3$) δ [ppm] 2.22 (tt, *J*= 6.72, 13.39 Hz, 2H), 2.54 (s, 3H), 2.88 (t, *J*= 6.59 Hz, 2H), 3.01 (br t, *J*= 14.34 Hz, 2H), 12.62 (br s, 1H).

6-Methyl-2-(methylthio)-5,6,7,8-tetrahydroquinazolin-4(3*H*)-one (4e). To a solution of 4-methylcyclohexanone (1.0 g, 8.92 mmol) and diethyl carbonate (10.8 mL) was added portionwise potassium t-butoxide at -10 °C. The reaction mixture was stirred for 2 hours at the same temperature and allowed to warm to ambient temperature. The reaction mixture was quenched with 1N aqueous hydrochloric acid and extracted twice with ethyl acetate. Combined organic layer was washed with water and saturated aqueous sodium chloride, dried over magnesium sulfate, filtered and evaporated under reduced pressure to give 1.01 g (62%, 5.48 mmol) of crude ethyl 5-methyl-2-cyclohexanonecarboxylate (**3e**) as an oil.

To a suspension of crude compound **3e** (1.0 g, 5.43 mmol) in water (10 mL) was added S-methylisothiourea sulfate (1.23 equiv, 1.86 g, 16.7 mmol) and potassium carbonate (2.4 equiv, 1.80 g, 13.0 mmol) at ambient temperature. The reaction mixture was stirred at 50 °C for 20 hours. The precipitate was collected, washed with water, and dried to give 440 mg (39%, 2.09 mmol) of compound **4e** as white powder; LC-MS (ESI) m/z 211 ($M + H^+$) observed for $C_{10}H_{14}N_2OS + H^+$. Retention time: 1.18 min. ^1H NMR (270 MHz, $CDCl_3$): δ [ppm] 1.07 (d, *J*= 6.59 Hz, 3H), 1.29-1.48 (m, 1H), 1.81-2.08 (m, 2H), 2.53-2.77 (m, 4H), 2.56 (s, 3H), 11.62-12.13 (m, 1H). Compounds **4c**, **4f**, and **4h** were prepared from the corresponding cyclic ketones (**2**) following the same procedure as compound **4e**.

2-(4-(2-Methoxyphenyl)-1,4-diazepan-1-yl)-5,6,7,8-tetrahydroquinazolin-4(3*H*)-one (7). 1-(2-Methoxyphenyl)-1,4-diazepane (**28**, 500 mg, 2.42 mmol), 1-amidinopyrazole hydrochloride (1.2 equiv, 426 mg, 2.91 mmol) and DIPEA (1.2 equiv, 0.51 mL, 2.91 mmol) in acetonitrile (10 mL) were stirred overnight at ambient temperature. The reaction mixture was filtered and the

precipitate was washed with acetonitrile and dried under reduced pressure to give 601 mg of compound **29** as a white solid (quant., 2.42 mmol); LC-MS (ESI) m/z 249 (M + H^+) observed for $C_{13}H_{20}N_4O$ + H^+. Retention time: 0.63 min.

To a suspension of compound **29** (1 equiv, 110 mg, 0.44 mmol) in EtOH (5 mL) was added compound **3a** (1.2 equiv, 100 mg, 0.53 mmol) and sodium ethoxide (1.5 equiv, 45.2 mg, 0.66 mmol) at ambient temperature. The reaction mixture was stirred for 20 hours, then diluted with water and chloroform, and extracted twice with chloroform. Combined organic layer was washed with water, dried over sodium sulfate, filtered and evaporated under reduced pressure. The residue was column chromatographed on silica gel (chloroform/methanol = 100:0–90:10) to give 67 mg (43%, 0.19 mmol) of compound **7** as white powder; LC-MS (ESI) m/z 355 (M + H^+). Retention time: 0.99 min. LC Purity: >99%. HRMS m/z (M + H^+) calculated for $C_{20}H_{26}N_4O_2$ + H^+: 355.2134, found: 355.2130. ^{1}H NMR (270 MHz, $CDCl_3$) δ [ppm] 1.64-1.80 (m, 4H), 2.03-2.14 (m, 2H), 2.36-2.51 (m, 4H), 3.22 (t, *J*= 5.28 Hz, 2H), 3.34-3.40 (m, 2H), 3.80 (t, *J*= 6.10 Hz, 2H), 3.85 (s, 3H), 3.86-3.94 (m, 2H), 6.83-6.99 (m, 4H), 10.20 (br s, 1H). Compounds **9**, **14**, **17**, and **18** were prepared from the corresponding intermediates **32**, **23**, **26**, and **27** following the same procedure as compound **7**, respectively.

2-(1-(2-Methoxyphenyl)piperidin-4-yl)-5,6,7,8-tetrahydroquinazolin-4(3*H*)-one (8). 1-(2-Methoxyphenyl)piperidine-4-carbonitrile (**30**, 226 mg, 1.05 mmol), hydroxylamine hydrochloride (6 equiv, 442 mg, 6.30 mmol) and potassium hydroxide (6.1 equiv, 359 mg, 6.41 mmol) in methanol (5 mL) were stirred for 30 min. The precipitate was filtered and washed with methanol (6 mL). The filtrate was stirred under reflux condition for 20 hours. The reaction mixture was evaporated under reduced pressure to use for the next reaction. Mixture of residue and 50% wet 10% Pd-Carbon (378 mg) in acetic acid (9 mL) and acetic anhydride (1 mL) were

stirred under hydrogen atmosphere (0.4 MPa) for 3days. The reaction mixture was filtered and evaporated to give 488 mg of crude compound **31** as a solid (quant., 1.05 mmol); LC-MS (ESI) m/z 234 (M + H^+) observed for $C_{13}H_{19}N_3O + H^+$. Retention time: 0.63 min.

To a solution of crude compound **31** (86 mg, 0.37 mmol) in THF (0.6 mL) and water (1 mL) was added compound **3a** (1.7 equiv, 79 mg, 0.63 mmol) and potassium carbonate (3 equiv, 123 mg, 1.11 mmol) at ambient temperature. The reaction mixture was stirred for 20 hours. Water and chloroform were added and the mixture was extracted four times with chloroform. Combined organic layer was washed with saturated sodium chloride, dried over sodium sulfate, filtered and evaporated under reduced pressure. The residue was column chromatographed on silica gel (chloroform/methanol = 100:0–90:10) to give 11.2 mg (9%, 0.033 mmol) of compound **8** as white powder; LC-MS (ESI) m/z 340 (M + H^+). Retention time: 0.99 min. LC Purity: >99%. HRMS m/z (M + H^+) calculated for $C_{20}H_{25}N_3O_2 + H^+$: 340.2025, found: 340.2017. ^{1}H NMR (270 MHz, $CDCl_3$) δ [ppm] 1.68-1.88 (m, 4H), 1.96-2.25 (m, 4H), 2.46-2.79 (m, 7H), 3.59 (d, *J*= 11.54 Hz, 2H), 3.83-3.92 (m, 3H), 6.84-7.07 (m, 4H), 11.78 (br s, 1H).

2-(Spiro[indoline-3,4'-piperidin]-1'-yl)-5,6,7,8-tetrahydroquinazolin-4(3*H*)-one (15). To a solution of 2-(methylthio)-5,6,7,8-tetrahydroquinazolin-4(3*H*)-one (**4a**, 1equiv, 75 mg, 0.38 mmol) in dichloromethane (3 mL) was added 70% *m*-chloroperbenzoic acid (1 equiv, 94 mg, 0.38 mmol) at -17 °C and stirred for 1.5 hours. The reaction mixture was evaporated and co-evaporated with DME (three times). A mixture of the residue, spiro[indoline-3,4'-piperidine] (**24**, 1.5 equiv, 153 mg, 0.57 mmol) and Et_3N (1.5 equiv, 80 μL, 0.57 mmol) in DME (2 mL) was stirred for 4 hours, then diluted with saturated sodium bicarbonate and ethyl acetate, and extracted three times with ethyl acetate. Combined organic layer was washed with water and saturated sodium chloride, dried over magnesium sulfate, evaporated under reduced pressure.

The residue was column chromatographed on silica gel (chloroform/methanol = 10:4) to give 158 mg (quant., 0.38 mmol) of compound **15** as a white solid; LC-MS (ESI) m/z 337 (M + H^+). Retention time: 0.97 min. LC Purity: >99%. HRMS m/z (M + H^+) calculated for $C_{20}H_{24}N_4O$ + H^+: 337.2029, found: 337.2023. ^{1}H NMR (400 MHz, DMSO-d_6) δ [ppm] 1.53-1.73 (m, 8H), 2.20-2.30 (m, 2H), 2.32-2.40 (m, 2H), 2.91-3.05 (m, 2H), 3.30 (s, 2H), 4.20-4.30 (m, 2H), 5.53 (s, 1H), 6.45-6.57 (m, 2H), 6.87-7.00 (m, 2H), 11.00 (br s, 1H).

Compounds **11-13**, **16**, and **52** (1N-Methyl **16**) were prepared from the corresponding compounds **20-22**, **25**, and 1N-Me **25** following the same procedure as compound **15**, respectively.

2-(4,6-Difluorospiro[indoline-3,4'-piperidin]-1'-yl)-5,6,7,8-tetrahydro-quinazolin-4(3*H*)-one (15c). To a solution of 1-benzyloxycarbonyl-4-formylpiperidine (1 equiv, 515 mg, 2.08 mmol) in chloroform (10 mL) was added 3,5-difluorophenylhydrazine (1 equiv, 0.25 mL, 2.08 mmol) and trifluoroacetic acid (3 equiv, 0.48 mL, 6.28 mmol) at ambient temperature. After stirring for 14 hours, sodium triacetoxyborohydride (2 equiv, 882 mg, 4.16 mmol) was added. After stirring for further 1 hour, the reaction mixture was quenched with saturated sodium bicarbonate, and extracted with chloroform. The organic layer was dried over magnesium sulfate, filtered and evaporated under reduced pressure. The residue was column chromatographed on silica gel (ethyl acetate/n-hexane = 50:50) to give 487 mg (65%, 1.36 mmol) of 1'-benzyloxycarbonyl-4,6-difluorospiro[indoline-3,4'-piperidine] (**38c**); LC-MS (ESI) m/z 359 (M + H^+) observed for $C_{20}H_{20}F_2N_2O_2$ + H^+.

To a solution of compound **38c** (1 equiv, 404 mg, 1.13 mmol) and di-tert-butyl dicarbonate (1.2 equiv, 295 mg, 1.35 mmol) in chloroform (5 mL) was added portionwise 4-dimethylaminopyridine (1.2 equiv, 165 mg, 1.35 mmol). The reaction mixture was stirred at

ambient temperature for 15 hours. The mixture was extracted with chloroform, washed with saturated sodium bicarbonate, water and saturated sodium chloride, dried over magnesium sulfate, filtered and evaporated under reduced pressure. The residue was column chromatographed on silica gel to give compound Boc-**38c**. Boc-**38c** and 10% Pd-Carbon (64 mg) in methanol (3 mL) was stirred under a hydrogen atmosphere at ambient temperature for 14 hours. The reaction mixture was filtered and evaporated to give 195 mg (quant., 1.13 mmol) of 1-tert-butyloxycarbonyl-4,6-difluorospiro [indoline-3,4'-piperidine] (Boc-**24c**).

Compound Boc-**24c** (1 equiv, 500 mg, 1.54 mmol), 1-amidinopyrazole hydrochloride (1.9 equiv, 426 mg, 2.91 mmol) and DIPEA (1.9 equiv, 0.5 mL, 2.91 mmol) in acetonitrile (10 mL) were stirred overnight at ambient temperature. The reaction mixture was filtered and the precipitate was washed with acetonitrile, dried under reduced pressure to give 601 mg of compound Boc-**34c** (quant., 1.54 mmol); LC-MS (ESI) m/z 367 ($M + H^+$) observed for $C_{18}H_{24}F_2N_4O_2 + H^+$. Retention time: 0.63 min.

To a suspension of crude compound Boc-**34c** (1 equiv, 110 mg, 0.30 mmol) in EtOH (5 mL) was added ethyl 2-cyclohexanone carboxylate (2 equiv, 100 mg, 0.59 mmol) and sodium ethoxide (2.2 equiv, 45.2 mg, 0.66 mmol) at ambient temperature. The reaction mixture was stirred for 20 hours. After addition of water, the mixture was extracted twice with chloroform. Combined organic layer was washed with water, dried over sodium sulfate, filtered and evaporated under reduced pressure. The residue was column chromatographed on silica gel (chloroform/methanol = 100:0–90:10) to give 67 mg of compound Boc-**15c** (43%, 0.14 mmol).

Compound Boc-**15c** (1 equiv, 49 mg, 0.10 mmol) in chloroform (1 mL) was cooled in an ice bath and trifluoroacetic acid (1 mL) was added. The reaction mixture was allowed to warm to ambient temperature and stirred for 3 hours. The mixture was quenched with saturated sodium

bicarbonate, extracted with ethyl acetate and washed with saturated sodium chloride. The organic layer was dried over sodium sulfate, filtered and concentrated to give 2 mg (5%, 0.005 mmol) of compound **15c** as a white solid: LC-MS (ESI) m/z 373 (M + H^+). Retention time: 1.20 min. LC Purity: 96.0%. HRMS m/z (M + H^+) calculated for $C_{20}H_{22}F_2N_4O$ + H^+: 373.1840, found: 373.1836. ^{1}H NMR (400 MHz, $CDCl_3$) δ [ppm] 1.66-1.78 (m, 4H), 1.80-1.86 (m, 2H), 2.19-2.28 (m, 2H), 2.36-2.41 (m, 2H), 2.45-2.50 (m, 2H), 2.93-3.02 (m, 2H), 3.60 (s, 2H), 3.98 (br s, 1H), 4.32-4.39 (m, 2H), 6.07-6.14 (m, 2H), 10.71 (br s, 1H).

Compounds **15a**, **15b**, **15d**, and **15e** were prepared from the corresponding starting materials following the same procedure as compound **15c**.

2-(4,6-Dichlorospiro[indoline-3,4'-piperidin]-1'-yl)-5,6,7,8-tetrahydroquinazolin-4(3*H*)-one (15f). Compound **38f** was prepared from the corresponding starting material following the same procedure as compound **38c**. Compound **38f** (1 equiv, 220 mg, 0.56 mmol) in trifluoroacetic acid (2 mL) was stirred under reflux condition for 3 hours. Trifluoroacetic acid was evaporated under reduced pressure. The residue was mixed with aqueous 1N aqueous sodium hydroxide and extracted three times with chloroform. The organic layer was dried over magnesium sulfate, filtered and evaporated under reduced pressure to give 58.3 mg (40%, 0.23 mmol) of crude 4,6-dichlorospiro[indoline-3,4'- piperidine] (**24f**) as a solid.

Compound **24f** (1 equiv, 58.3 mg, 0.23 mmol), 1-amidinopyrazole (1.5 equiv, 50 mg, 0.34 mmol) and Et_3N (3 equiv, 0.1 mL, 0.72 mmol) in acetonitrile (2 mL) were stirred at 50 °C for 2 hours. The reaction mixture was concentrated to give crude 4,6-dichlorospiro[indoline-3,4'-piperidine]-1'-carboximidamide (**34f**).

To a suspension of crude compound **34f** in EtOH (2 mL) was added ethyl 2-cyclohexanone carboxylate (1.2 equiv, 46 mg, 0.27 mmol) and sodium ethoxide (2.9 equiv, 46 mg, 0.68 mmol)

at ambient temperature. The reaction mixture was stirred at 70 °C for 3 hours and water and chloroform were added. The mixture was extracted twice with chloroform and combined organic layer was washed with water, dried over sodium sulfate, filtered and evaporated. The residue was column chromatographed on silica gel (chloroform/methanol = 95:5) to give 71.2 mg (78%, 0.18 mmol) of compound **15f** as white powder; LC-MS (ESI) m/z 405 (M + H^+). Retention time: 1.30 min. LC Purity: >99%. HRMS m/z (M + H^+) calculated for $C_{20}H_{22}Cl_2N_4O$ + H^+: 405.1249, found: 405.1243. ^{1}H NMR (400 MHz, DMSO-d_6) δ [ppm] 1.55-1.70 (m, 6H), 2.20-2.45 (m, 6H), 2.80-2.95 (m, 2H), 3.55 (s, 2H), 4.25-4.40 (m, 2H), 6.33 (br s, 1H), 6.42 (d, *J*= 2.0 Hz, 1H), 6.49 (d, *J*= 2.0 Hz, 1H), 11.04 (br s, 1H).

Compound **15g** was prepared from the corresponding starting material following the same procedure as compound **15f**.

1'-(4-Oxo-3,4,5,6,7,8-hexahydroquinazolin-2-yl)spiro[indoline-3,4'-piperidine]-4-carbonitrile (15h). Compound **15h** (193 mg, 93%, 0.53 mmol) as white powder was obtained from spiro[indoline-3,4'-piperidine]-4-carbonitrile (**24h**) following the same procedure as compound **15f**; LC-MS (ESI) m/z 362 (M + H^+). Retention time: 1.11 min. LC Purity: 98.5%. HRMS m/z (M + H^+) calculated for $C_{21}H_{23}N_5O$ + H^+: 362.1981, found: 362.1972. ^{1}H NMR (400 MHz, $CDCl_3$) δ [ppm] 1.64-1.86 (m, 6H), 2.33-2.39 (m, 2H), 2.42-2.52 (m, 4H), 2.91-3.00 (m, 2H), 3.65 (s, 2H), 4.02 (br s, 1H), 4.53-4.60 (m, 2H), 6.79 (d, *J*= 7.8 Hz, 1H), 6.95 (d, *J*= 7.6 Hz, 1H), 7.07-7.12 (m, 1H), 11.89 (br s, 1H).

4-Fluoro-1'-(4-oxo-3,4,5,6,7,8-hexahydroquinazolin-2-yl)spiro[indoline-3,4'-piperidin]-2-one (16a). To a solution of 1-benzyloxycarbonyl-4-formylpiperidine (1 equiv, 567 mg, 2.29 mmol) in chloroform (4.6 mL) was added 3-fluorophenylhydrazine hydrochloride (1.5 equiv, 560 mg, 3.44 mmol) and trifluoroacetic acid (3 equiv, 0.53 mL, 6.93 mmol) at ambient

temperature. The mixture was heated at 60 °C for 1 hour and cooled down to ambient temperature. The reaction mixture was quenched with saturated sodium bicarbonate, extracted with chloroform and washed with saturated sodium chloride. The organic layer was dried over sodium sulfate, filtered and evaporated under reduced pressure. The residue was column chromatographed on silica gel (ethyl acetate/n-hexane = 50:50) to give 424 mg of less polar element and 202 mg of more polar element. The latter (1 equiv, 202 mg, 0.60 mmol) was dissolved in chloroform (5.7 mL) and manganese (IV) oxide (27 equiv, 1.41 g, 16.2 mmol) was added. After stirring at ambient temperature for 20 hours, the mixture was filtered through celite pad and washed with chloroform. The filtrate was concentrated and column chromatographed on silica gel (ethyl acetate/n-hexane = 50:50) to give 137 mg (17%, 0.39 mmol) of 1'-benzyloxycarbonyl-4-fluorospiro[indoline-3,4'-piperidin]-2-one (**39a**); LC-MS (ESI) m/z 355 (M + H^+) observed for $C_{20}H_{19}FN_2O_3$ + H^+.

The less polar element obtained above (1 equiv, 424 mg, 1.25 mmol) was dissolved in chloroform (12 mL) and manganese (IV) oxide (28 equiv, 3.05 g, 35.1 mmol) was added. After stirring at ambient temperature for 60 hours, the mixture was filtered through a celite pad and washed with chloroform. The filtrate was concentrated and column chromatographed on silica gel (ethyl acetate/n-hexane = 50:50) to give 165 mg (20%, 0.47 mmol) of 1'-benzyloxy carbonyl-6-fluorospiro[indoline-3,4'-piperidin]-2-one (**39b**); LC-MS (ESI) m/z 355 (M + H^+) observed for $C_{20}H_{19}FN_2O_3$ + H^+.

To a solution of 1'-benzyloxycarbonyl-4-fluorospiro[indoline-3,4'-piperidin]-2-one (**39a**) (1 equiv, 137 mg, 0.39 mmol) in chloroform (0.8 mL) was added di-tert-butyl dicarbonate (1.5 equiv, 127 mg, 0.58 mmol) and 4-dimethylaminopyridine (0.5 equiv, 25 mg, 0.20 mmol) at ambient temperature. After stirring for 18 hours, saturated sodium bicarbonate was added,

extracted with chloroform and washed with saturated sodium chloride. The organic layer was dried over sodium sulfate, filtered and evaporated under reduced pressure. The residue was column chromatographed on silica gel (ethyl acetate/n-hexane = 20:80) to give 133 mg (75%, 0.29 mmol) of 1'-benzyloxycarbonyl-1-tert-butoxycarbonyl-4-fluorospiro[indoline-3,4'-piperidin]-2-one; LC-MS (ESI) m/z 455 (M + H^+) observed for $C_{25}H_{27}FN_2O_5$ + H^+.

This compound and 10% Pd-Carbon (15 mg) in methanol (2.9 mL) were stirred under a hydrogen atmosphere at ambient temperature for 63 hours. The reaction mixture was filtered through a celite pad and washed with methanol. The filtrate was concentrated and column chromatographed on silica gel (ethyl acetate/n-hexane = 50:50) to give 47.9 mg (51%, 0.15 mmol) of 1-tert-butoxycarbonyl-4-fluorospiro[indoline-3,4'-piperidin]-2-one (Boc-**25a**); LC-MS (ESI) m/z 321 (M + H^+) observed for $C_{17}H_{21}FN_2O_3$ + H^+.

A solution of this compound (1 equiv, 54.9 mg, 0.17 mmol) in chloroform (0.14 mL) was cooled in an ice bath and trifluoroacetic acid (10 equiv, 0.14 mL, 1.83 mmol) was added. The reaction mixture was warmed up to ambient temperature and stirred for 3 hours. The mixture was quenched with saturated sodium bicarbonate, extracted with ethyl acetate and washed with saturated sodium chloride. The organic layer was dried over sodium sulfate, filtered and concentrated to give 7.3 mg (19%, 0.033 mmol) of 4-fluorospiro[indoline-3,4'-piperidin]-2-one (**25a**); LC-MS (ESI) m/z 221 (M + H^+) observed for $C_{12}H_{13}FN_2O$ + H^+.

Compound **25a** (7.3 mg, 0.033 mmol), 1-amidinopyrazole hydrochloride (1.06 equiv, 5.1 mg, 0.035 mmol) and Et_3N (3 equiv, 0.014 mL, 0.10 mmol) in EtOH (0.2 mL) were stirred overnight at ambient temperature. The reaction mixture was concentrated to give crude compound **35a**. To a suspension of compound **35a** in EtOH (0.2 mL) was added ethyl 2-cyclohexanonecarboxylate (1.15 equiv, 6.4 mg, 0.038 mmol) and sodium ethoxide (3 equiv, 6.8

mg, 0.10 mmol) at ambient temperature and stirred for 4 days. The reaction mixture was concentrated and purified by PLC (chloroform/methanol = 90:10) to give 7.2 mg (59%, 0.019 mmol) of compound **16a** as white powder; LC-MS (ESI) m/z 369 (M + H^+). Retention time: 1.12 min. LC Purity: >99%. HRMS m/z (M + H^+) calculated for $C_{20}H_{21}FN_4O_2$ + H^+: 369.1727, found: 369.1725. ^{1}H NMR (400 MHz, DMSO-d_6) δ [ppm] 1.54-1.72 (m, 4H) 1.73-1.85 (m, 2H) 1.94-2.05 (m, 2H) 2.19-2.29 (m, 2H) 2.35-2.42 (m, 2H) 3.67-3.81 (m, 2H) 4.00-4.16 (m, 2H) 6.71 (d, *J*= 7.58 Hz, 1H) 6.73-6.80 (m, 1H) 7.19-7.27 (m, 1H) 10.65 (s, 1H).

6-Fluoro-1'-(4-oxo-3,4,5,6,7,8-hexahydroquinazolin-2-yl)spiro[indoline-3,4'-piperidin]-2-one (16b). Trifluoroacetic acid (64 equiv, 2.3 mL, 30.0 mmol) was added to 1'-benzyloxycarbonyl-6- fluorospiro[indoline-3,4'-piperidin]-2-one (**39b**, 1 equiv, 165 mg, 0.47 mmol) and heated at 80 °C for 3 hours. The reaction mixture was cooled to 0 °C and made alkaline with sodium hydroxide solution, extracted with chloroform and washed with saturated sodium chloride. The organic layer was dried over sodium sulfate, filtered and evaporated under reduced pressure. The residue was column chromatographed on amino silica gel (methanol/chloroform = 15:85) to give 65.4 mg (64%, 0.30 mmol) of 6-fluorospiro[indoline-3,4'-piperidin]-2-one (**25b**); LC-MS (ESI) m/z 221 (M + H^+) observed for $C_{12}H_{13}FN_2O$ + H^+.

Compound **16b** (25.2 mg, 25%, 0.068 mmol) was prepared from compound **25b** following the same procedure as compound **16a**; white powder; LC-MS (ESI) m/z 369 (M + H^+). Retention time: 1.11 min. LC Purity: 96.3%. HRMS m/z (M + H^+) calculated for $C_{20}H_{21}FN_4O_2$ + H^+: 369.1727, found: 369.1724. ^{1}H NMR (400 MHz, $CDCl_3$) δ [ppm] 1.52-1.78 (m, 8H) 2.20-2.31 (m, 2H) 2.35-2.42 (m, 2H) 3.80-4.00 (m, 4H) 6.64-6.69 (m, 1H) 6.70-6.77 (m, 1H) 7.51 (dd, *J*= 8.31, 5.50 Hz, 1H) 10.57 (s, 1H) 11.05 (br s., 1H).

Compounds **16c**, **16d**, **16e**, **16f**, and **16g** were prepared from the corresponding starting materials following the same procedure as compound **16b**.

2-Oxo-1'-(4-oxo-3,4,5,6,7,8-hexahydroquinazolin-2-yl)spiro[indoline-3,4'-piperidine]-4-carbonitrile (16h). Compound **16h** (8.0 mg, 19%, 0.021 mmol) was prepared from 2-oxospiro[indoline- 3,4'-piperidine]-4-carbonitrile (**25h**) following the procedure for compound **16a**; white powder; LC-MS (ESI) m/z 376 (M + H^+). Retention time: 1.09 min. LC Purity: >99%. HRMS m/z (M + H^+) calculated for $C_{21}H_{21}N_5O_2$ + H^+: 376.1773, found: 376.1767. ^{1}H NMR (400 MHz, DMSO-d_6) δ [ppm] 1.60-1.79 (m, 6H), 2.21-2.30 (m, 4H), 2.37-2.42 (m, 2H), 3.58-3.67 (m, 2H), 4.24-4.35 (m, 2H), 7.17 (dd, *J*= 6.4, 2.6 Hz, 1H), 7.37-7.43 (m, 2H), 10.82 (br s, 1H), 11.12 (br s, 1H).

2-(4-Fluoro-1-(2-hydroxyethyl)spiro[indoline-3,4'-piperidin]-1'-yl)-5,6,7,8-tetrahydroquinazolin-4(3*H*)-one (40a). To a suspension of sodium hydride (55% in oil, 2.7 equiv, 32.4 g, 0.74 mmol) in DMF (400 mL) was added 2-(2,6-difluorophenyl)acetonitrile (1 equiv, 41.4 g, 0.27 mmol) under ice cooling. Benzyl bis(2-chloroethyl)amine (1 equiv, 62.7 g, 0.27 mmol) in DMF (50 mL) was added and the mixture was allowed to be stirred at ambient temperature and heated at 55 °C for 2 hours. After reaction was completed, the mixture was quenched with ice water and diluted with ethyl acetate, water and 1M aqueous citric acid (3 mL). The aqueous layer was extracted three times with ethyl acetate. Combined organic layer was washed with saturated aqueous sodium chloride, dried over magnesium sulfate, filtered and evaporated under reduced pressure. The residue was crystalized from heptane to give 71.8 g (86%, 0.23 mmol) of 1-benzyl-4-(2,6-difluorophenyl)piperidine-4-carbonitrile (**45a**). LC-MS (ESI) m/z 313 (M + H^+) observed for $C_{19}H_{18}F_2N_2$ + H^+.

95% sulfuric acid (10 equiv, 9.0 mL, 160 mmol) was added to compound **45a** (1 equiv, 5 g, 16 mmol) and the reaction mixture was stirred at 80 °C for 30 minutes. The reaction mixture was added dropwise to a solution of potassium carbonate (20 equiv, 44.2 g, 320 mmol), water (50 mL), ice (50 g) and ethyl acetate (100 mL). The mixture was extracted with ethyl acetate and combined organic layer was washed with saturated sodium chloride, dried over sodium sulfate, filtered and evaporated under reduced pressure. The residue was treated with ethyl acetate/heptane for crystallization to give 3.45 g (65%, 10.5 mmol) of 1-benzyl-4-(2,6-difluorophenyl)piperidine-4-carboxamide.

Lithium hydride (2.1 equiv, 0.18 g, 22.6 mmol) was added to a solution of this carboxamide (1 equiv, 3.45 g, 10.5 mmol) in N-methylpyrrolidone (64 mL) under an argon atmosphere and ice cooling. The reaction mixture was stirred at 80–120 °C for 3.5 hours and added to a mixture of ethyl acetate, water and ice. The aqueous layer was separated and extracted three times with ethyl acetate. Combined organic layer was washed with water (twice) and saturated sodium chloride, dried over sodium sulfate, filtered, and evaporated under reduced pressure. The residue was treated with ethyl acetate/heptane for crystallization to give 2.25 g (69%, 7.26 mmol) of 1'-benzyl-4-fluorospiro[indoline-3,4'-piperidin]-2-one (**46a**). LC-MS (ESI) m/z 311 ($M + H^+$) observed for $C_{19}H_{19}FN_2O + H^+$.

To a suspension of lithium aluminum hydride (4 equiv, 0.49 g, 12.9 mmol) in THF (13 mL) was added portionwise compound **46a** (1 equiv, 1.0g, 3.21 mmol) under an argon atmosphere and ice cooling. The reaction mixture was allowed to warm to ambient temperature and stirred under reflux condition for 15 hours. Ethyl acetate, water, 15% sodium hydroxide, and water were added to the mixture. The mixture was stirred for 30 minutes, filtered with celite, and washed with 10% methanol in chloroform. The filtrate was evaporated and the residue was treated with

ethyl acetate/heptane to give 608 mg (64%, 2.05 mmol) of 1'-benzyl-4-fluoro-spiro[indoline-3,4'-piperidine] (**47a**). LC-MS (ESI) m/z 297 (M + H^+) observed for $C_{19}H_{21}FN_2$ + H^+.

Compound **47a** (1equiv, 220 mg, 0.74 mmol) and ethylenebromohydrin (4 equiv, 371 mg, 2.97 mmol) were dispensed in a sealed microwave vessel (2-5 mL) in THF (4 mL). The mixture was heated at 130 ℃ for 4 hours with microwave irradiation. The reaction mixture was concentrated and purified by PLC eluted with DCM:MeOH (v/v = 95:5) to give 200 mg (79%, 0.59 mmol) of 2-(1'-benzyl-4-fluorospiro[indoline-3,4'-piperidin]-1-yl)ethanol (**48a**) as yellow oil. LC-MS (ESI) m/z 341.4 (M + H^+) observed for $C_{21}H_{25}FN_2O$ + H^+. ^{1}H NMR (270 MHz, $CDCl_3$), δ: 1.35-2.09 (m, 4H), 3.05-3.36 (m, 6H), 3.40 (s, 2H), 3.60-3.74 (m, 1H), 3.77-3.90 (m, 2H), 3.96-4.30 (m, 2H), 6.13-6.44 (m, 2H), 6.95-7.14 (m, 1H), 7.53-7.78 (m, 3H),7.56-7.71 (m, 2H).

20% $Pd(OH)_2$-Carbon (0.1 equiv, 82.5 mg, 0.059 mmol) was added to compound **48a** (1 equiv, 200 mg, 0.59 mmol) in EtOH (3 mL). The mixture was stirred at ambient temperature under an atmosphere of H_2 for 19 hours. The mixture was filtered through a pad of celite. The filtrate was concentrated to give 150 mg (quant., 0.59 mmol) of 2-(4-fluorospiro[indoline-3,4'-piperidin]-1-yl)ethanol (**49a**) without further purification. LC-MS (ESI) m/z 251 (M + H^+) observed for $C_{14}H_{19}FN_2O$ + H^+.

2-Chloro-5,6,7,8-tetrahydroquinazolin-4(3*H*)-one (1 equiv, 23.7 mg, 0.13 mmol), compound **49a** (1 equiv, 33.5 mg, 0.13 mmol) and Et_3N (1 equiv, 12.8 mg, 0.13 mmol) were dispensed in a sealed microwave vessel (2-5 mL) in EtOH (4 mL). The mixture was heated at 150 °C for 30 minutes with microwave irradiation. The reaction mixture was concentrated and purified by PLC eluted with DCM:MeOH (v/v = 10:1) to give 13.6 mg (27%, 0.034 mmol) of compound **40a** as a clear solid. LC-MS (ESI) m/z 399 (M + H^+). Retention Time: 1.16 min.

Purity: 95.2 %. HRMS m/z (M + H^+) calculated for $C_{22}H_{27}FN_4O_2$ + H^+: 399.2196, found: 399.2191. ^{1}H NMR (270 MHz, $CDCl_3$), δ: 1.73-1.85 (m, 8H), 2.24-2.62 (m, 6H), 2.88-3.05 (m, 2H), 3.33 (t, *J*= 5.4 Hz, 2H), 3.48 (s, 2H), 3.84 (t, *J*= 5.4 Hz, 2H), 6.31-6.41 (m, 2 H), 7.01-7.26 (m, 1H).

2-(4,6-Difluoro-1-(2-hydroxyethyl)spiro[indoline-3,4'-piperidin]-1'-yl)-5,6,7,8-tetrahydroquinazolin-4(3*H*)-one (40c). To a solution of 2-(4,6-difluorospiro[indoline-3,4'-piperidin]-1'-yl)-5,6,7,8-tetrahydroquinazolin-4(3*H*)-one (**15c**) (1 equiv, 31.8 mg, 0.085 mmol) in chloroform (1 mL) was added glycolaldehyde dimer (1.5 equiv, 15.4 mg, 0.128 mmol), sodium triacetoxyborohydride (3 equiv, 54.3 mg, 0.256 mmol) and acetic acid (20 equiv, 0.1 mL, 1.75 mmol) at ambient temperature. After stirring at reflux for 14 hours, the reaction mixture was quenched with saturated sodium bicarbonate and extracted with chloroform. The organic layer was dried over magnesium sulfate, filtered and evaporated under reduced pressure. The residue was column chromatographed on silica gel (methanol/chloroform = 10:90) to give 12.4 mg (35%, 0.030 mmol) of **40c** as an off-white solid; LC-MS (ESI) m/z 417 (M + H^+). Retention time: 1.16 min. LC Purity: >99%. HRMS m/z (M + H^+) calculated for $C_{22}H_{26}F_2N_4O_2$ + H^+: 417.2102, found: 417.2098. ^{1}H-NMR (400 MHz, $CDCl_3$) δ: 1.64-1.83 (m, 6H), 2.20-2.30 (m, 2H), 2.33-2.38 (m, 2H), 2.45-2.50 (m, 2H), 2.91-3.00 (m, 2H), 3.30 (t, *J*= 5.4 Hz, 2H), 3.54 (s, 2H), 3.84 (t, *J*= 5.4 Hz, 2H), 4.42-4.49 (m, 2H), 6.00-6.09 (m, 2H), 11.69 (br s, 1H).

Compounds **40**, **40d**, and **40f** were prepared from compounds **15**, **15d**, and **15f** following the same procedure as compound **15c**.

4-Fluoro-1-(2-hydroxyethyl)-1'-(4-oxo-3,4,5,6,7,8-hexahydroquinazolin-2-yl)spiro[indoline-3,4'-piperidin]-2-one (43a). 1'-Benzyl-4-fluorospiro[indoline-3,4'-piperidin]-2-one (**46a**, 1 equiv, 300 mg, 0.97 mmol), ethylenebromohydrin (3 equiv, 360 mg, 2.90 mmol) and potassium

carbonate (3 equiv, 400 mg, 2.90 mmol) were dispensed in a sealed tube in DMF (2 mL) and the mixture was stirred at 70 °C for 2 hours. The crude product was extracted with DCM (50 mL) and washed with H_2O (10 mL). The organic layer was separated and concentrated, and the residue was purified by column chromatography on a silica gel and eluted with mixtures of hexane:EtOAc (v/v = 3:1 and 1:1) to give 200 mg (58%, 0.57 mmol) of 1'-benzyl-4-fluoro-1-(2-hydroxyethyl)spiro[indoline-3,4'-piperidin]-2-one (**50a**) as a clear solid. LC-MS (ESI) m/z 355 (M + H^+) observed for $C_{21}H_{23}FN_2O_2$ + H^+.

20% $Pd(OH)_2$ on carbon (0.1 equiv, 79.2 mg, 0.056 mmol) was added to compound **50a** (1 equiv, 200 mg, 0.56 mmol) in EtOH (4 mL). The mixture was stirred at ambient temperature under an atmosphere of H_2 for 3 hours. The mixture was concentrated and purified by PLC eluted with DCM:MeOH:28% aqueous NH_3 (v/v = 100:10:2) to give 63.2 mg (42%, 0.24 mmol) of 4-fluoro-1-(2-hydroxyethyl)spiro[indoline-3,4'-piperidin]-2-one (**42a**). LC-MS (ESI) m/z 265 (M + H^+) observed for $C_{14}H_{17}FN_2O_2$ + H^+. ^{1}H NMR (270 MHz, $CDCl_3$), δ: 1.66-1.96 (m, 2H), 2.07-2.28 (m, 2H), 2.96-3.10 (m, 2H), 3.39-3.57 (m, 2H), 3.73-3.95 (m, 4H), 6.60-6.82 (m, 2H), 7.11-7.27 (m, 1H).

2-Chloro-5,6,7,8-tetrahydroquinazolin-4(3*H*)-one (**51**, 1equiv, 18.3 mg, 0.098 mmol), compound **42a** (1 equiv, 26.0 mg, 0.098 mmol) and Et_3N (1 equiv, 10.0 mg, 0.098 mmol) were dispensed in a sealed microwave vessel (2-5 mL) in EtOH (4 mL). The mixture was heated at 150 °C for 30 minutes with microwave irradiation. The reaction mixture was concentrated and purified by PLC eluted with DCM:MeOH (v/v = 95:5) to give 13.9 mg (34%, 0.034 mmol) of compound **43a** as a clear solid; LC-MS (ESI) m/z 413 (M + H^+). Retention Time: 1.10 min. Purity; >99%. HRMS m/z (M + H^+) calculated for $C_{22}H_{25}FN_4O_3$ + H^+: 413.1989, found:

413.1979. ^{1}H NMR (270 MHz, $CDCl_3$), δ: 1.68-1.90 (m, 6H), 2.25-2.54 (m, 6H), 3.87-3.99 (m, 6H), 4.23-4.29 (m, 2H), 6.71-6.77 (m, 2H), 7.21-7.26 (m, 1H).

Compound **43** was prepared from compound **42** following the same procedure as compound **43a**.

4,6-Difluoro-1-(2-hydroxyethyl)-1'-(4-oxo-3,4,5,6,7,8-hexahydroquinazolin-2-yl)spiro[indoline-3,4'-piperidin]-2-one (43c). To a solution of compound **39c** (1 equiv, 60.0 mg, 0.16 mmol) in DMF (1 mL) was added 2-(2-chloroethoxy)tetrahydro-2*H*-pyran (3 equiv, 0.07 mL, 0.47 mmol), sodium hydride (60%, dispersion in paraffin liquid) (3 equiv, 19.3 mg, 0.48 mmol) and sodium iodide (1 equiv, 24.2 mg, 0.16 mmol) at ambient temperature. After stirring at 80 °C for 14 hours, the reaction mixture was quenched with saturated ammonium chloride and extracted with ethyl acetate. The organic layer was dried over magnesium sulfate, filtered and evaporated under reduced pressure. To the residue was added methanol (1 mL) and p-toluene sulfonic acid monohydrate (0.1 equiv, 3.0 mg, 0.016 mmol). After stirring at ambient temperature for 1 hour, the reaction mixture was quenched with saturated sodium bicarbonate and extracted with chloroform. The organic layer was dried over magnesium sulfate, filtered and evaporated under reduced pressure. The residue was column chromatographed on silica gel (ethyl acetate/n-hexane = 80:20) to give 16.1 mg (24%, 0.039 mmol) of 1'-benzyloxycarbonyl-4,6-difluoro-1-(2-hydroxyethyl) spiro[indoline-3,4'-piperidin]-2-one (**41c**); LC-MS (ESI) m/z 417 (M + H^+) observed for $C_{22}H_{22}F_2N_2O_4$ + H^+.

Compound **41c** (1 equiv, 1.04 g, 2.49 mmol) in trifluoroacetic acid (53 equiv, 10 mL, 131 mmol) was stirred at reflux for 3 hours. Trifluoroacetic acid was evaporated under reduced pressure. The residue was mixed with aqueous 5N sodium hydroxide and extracted with chloroform. The organic layer was dried over magnesium sulfate, filtered and evaporated under

reduced pressure to give crude 4,6-difluoro-1-(2-hydroxyethyl)spiro[indoline-3,4'-piperidin]-2-one (**42c**).

Crude compound **42c**, 1-amidinopyrazole hydrochloride (1.2 equiv, 439 mg, 2.99 mmol) and Et_3N (3 equiv, 1.04 mL, 7.68 mmol) in acetonitrile (20 mL) were stirred at ambient temperature for 1 hour. After removal of the solvent, the residue was dissolved in EtOH (20 mL). Ethyl 2-cyclohexanonecarboxylate (1.2 equiv, 0.48 mL, 3.0 mmol) and 21% sodium ethoxide in EtOH (3 equiv, 2.43 mL, 7.49 mmol) was added at ambient temperature. After stirred at reflux for 3 hours, the reaction mixture was quenched with saturated sodium bicarbonate and extracted with chloroform. The organic layer was dried over magnesium sulfate, filtered and evaporated under reduced pressure. The residue was column chromatographed on silica gel (methanol/chloroform = 10:90) to give 589 mg (55%, 1.37 mmol) of compound **43c** as white powder; LC-MS (ESI) m/z 431 ($M + H^+$). Retention Time: 1.10 min. Purity: 98.1%. HRMS m/z ($M + H^+$) calculated for $C_{22}H_{24}F_2N_4O_3 + H^+$: 431.1895, found: 431.1891. ^{1}H-NMR (400 MHz, $CDCl_3$) δ: 1.65-1.78 (m, 4H), 1.82-1.89 (m, 2H), 2.22-2.31 (m, 2H), 2.34-2.39 (m, 2H), 2.45-2.50 (m, 2H), 3.83-3.94 (m, 6H), 4.19-4.26 (m, 2H), 6.45-6.50 (m, 1H), 6.56 (dd, *J*= 8.6, 2.0 Hz, 1H), 10.70 (br s, 1H).

Compounds **43d** and **43f** were prepared from compounds **39d** and **39f** following the same procedure as compound **43c**, respectively.

Physicochemical and biochemical properties evaluation

Aqueous solubility (Aq. Sol., pH7.4). Direct UV kinetic solution method was performed. A 10mM DMSO solution of compound is added to the micro-tube containing aqueous pH 7.4 phosphate buffer solution (Maximum concentration: 200 μM). The solution mixture was vigorously shaken at ambient temperature for 1 hour. Precipitate was removed by centrifugal

separation, and the UV absorbance of the supernatant and the standard solution prepared by test compound for calibration was measured in duplicate using a 96 well UV plate reader, SPECTRA MAX190 (Molecular Devices, Japan).

Parallel Artificial Membrane Permeability Assay (PAMPA). Parallel artificial membrane permeability measurements were performed in duplicate with BD Gentest™ Pre-coated PAMPA Plate System according to the standard protocol of BD Bioscience (Bedford MA, US).

Serum Protein Binding assay (Hu/Mo PB). Serum protein binding analyses were performed in Sumika Chemical Analysis Service, Ltd. (SCAS) with Harvard Apparatus Fast Micro-Equilibrium DIALYZER™ according to the standard protocol of Harvard Apparatus (Holliston MA, US). For each experiment, 1μM of test compound was used and after 24 hours of equilibrium time, concentrations of donor and acceptor layer were determined by LC-MS/MS analysis.

Liver microsomal stability assay (Hu/Mo Mics.Stab.). Liver microsome analyses (Human, Mouse) were performed in RIKEN or SCAS according to the standard protocols[45]. For each experiment, 1μM of substrate, 0.5 mg protein/ml of microsome and 3.5μM β-NADPH was used, and remaining substrate after 30minutes incubation was determined by LC-MS/MS analysis.

P-glycoprotein efflux assay (MDCKII, MDR1-MDCKII). P-gp analyses were performed in SCAS according to the standard protocols[37].

Pharmacokinetic Analysis. The pharmacokinetic (PK) analyses of mouse intraperitoneal (ip, 50 mg/kg), rat per oral (po, 1 mg/kg) and intravenous (iv, 3 mg/kg) injections were performed in Meiji Seika pharmaceutical Co. Ltd., and Nemoto science Co. Ltd. according to the standard protocols under previous approval from the Animal Care and Ethic Committee of these companies. The ip formulation was prepared from DMSO/HCO-40/EtOH/Cremophor-EL/saline

(5:12.5:12.5:20:50) cocktail solution. The iv formulation was prepared from DMSO/PEG400/saline (10:40:50). The po formulation was water suspension in 0.5 w/v% methylcellulose 400 in saline.

Biological Evaluation

Preparation of tankyrase and PARP family proteins. Tankyrase-1 (TNKS) and -2 (TNKS2) proteins were prepared by the method described in previous paper.[42] Human PARP1 and PARP2 were purchased from Trevigen, Gaithersburg, MD 20877 and Bioscience, San Diego, CA 92121 USA, respectively. The catalytic domain of human PARP10 (residues 818–1025) containing a modified natural poly-histidine (N11; MKDHLIHNHHKHEHAHAEH) affinity tag, a FLAG tag and a tobacco etch virus (TEV) protease cleavage site at the N-terminus, was synthesized using the Escherichia coli cell-free protein synthesis system. The synthesized PARP10 was affinity-purified by chromatography on a HisTrap HP column (GE Healthcare Biosciences, Chicago, IL, USA), and eluted with 20 mM Tris–HCl buffer (pH 8.0) containing 500 mM NaCl and 500 mM imidazole. The eluted fractions were further purified by size-exclusion column chromatography using a HiLoad 16/60 Superdex 75 column (GE Healthcare Biosciences) equilibrated in 20 mM Tris–HCl buffer (pH 8.0) containing 150 mM NaCl and 10% glycerol.

ELISA for tankyrases, PARP1, PARP2, and PARP10. To measure poly (ADP-ribosyl)ation activity of tankyrases, tankyrase-1 (TNKS) and -2 (TNKS2) proteins were prepared and ELISA was performed by the method described in the previous paper.[42] To measure poly- or mono(ADP-ribosyl)ation activity of PARP1, PARP2, or PARP10, histone was used as a substrate to perform a colorimetric ELISA method. Histone (50 μl of 0.1 mg/ml in phosphate-buffered saline (PBS)) was covalently bound to maleimide-activated plates (ThermoFisher Scientific) at 4°C for overnight. After washing the plates four times with 200 μl of washing

buffer (PBS containing 0.1% Triton X-100), 300 μl of L-cysteine-hydrochloride solution (10 μg/ml in PBS) was added. After 1 h at room temperature, the plates were washed four times with 200 μl of washing buffer. Then, PARP assay was carried out in 50 μl reaction mixture (50 mM Tris-HCl (pH 8.0), 4 mM $MgCl_2$, 0.2 mM DTT, 0.5 μl compound (dissolved in DMSO), PARP protein, 25 μM NAD^+ containing10% biotinylated-NAD^+ (Trevigen)) at 30°C for 45 min. For PARP1 or PARP2 assay, one unit of human PARP1 or 0.52 μg of human PARP2 was used and activated DNA was added into the reaction mixture. For PARP10, 0.2 μg of human PARP10 was used. After washing the plates four times with 200 μl of washing buffer, 50 μl of Streptavidin-HRP (1:1000, diluted in L-cysteine-hydrochloride solution) was added. After 20 min at room temperature, plates were washed four times with 200 μl of washing buffer and 50 μl of TACS-Sapphire™ (Trevigen) was added. After 5- ~ 20-min incubation at room temperature, color development was monitored. The plates were read at 630 nm or at 450 nm after the reaction was stopped by adding 0.2 N HCl using a SpectraMax M2^e microplate reader (Molecular Devices). A blank value (in the absence of enzyme) was subtracted before calculating percent inhibition.

Cell culture. A human colorectal cancer cell line COLO-320DM was maintained in RPMI1640 medium (Nacalai Tesque or Wako) with 10% heat-inactivated FBS (fetal bovine serum) and 100 μg/mL kanamycin or 100 U/mL Penicillin/100 μg/mL Streptomycin if necessary. Human colorectal cancer cell lines RKO and DLD-1 and human embryonic kidney cell line HEK293 were maintained in DMEM medium (Wako or Nacalai Tesque) with 10% FBS and, if necessary, 100 U/mL Penicillin/100 μg/mL Streptomycin. Human colorectal cancer cell lines were obtained from the American Type Culture Collection (Manassas, VA, USA).

TCF reporter assay. DLD-1 and HEK293 cells were transfected with the β-catenin-responsive reporter vectors pTcf7wt-luc (carrying 7 repeats of the Tcf-binding consensus sequence upstream

of the lucifearse gene) (provided by Dr. Kunitada Shimotohno, National Center for Global Health and Medicine, via RIKEN BioResource Center, Ibaraki, Japan) by FuGENE HD transfection reagent (Promega). For HEK293 cells, Wnt3A conditioned medium was used to activate the Wnt pathway. Transfected cells were treated with various concentrations of tested compounds for 24 h. Luciferase assay was performed using the Pikka-gene assay system (TOYO B-Net) and luminescence was measured using a SynergyH4 microplate reader (BioTek).

COLO-320DM cell growth inhibition CellTiter-Glo assay. To evaluate cell viability, CellTiter-Glo® reagent was used after treatment of cells with compounds at a final DMSO concentration of 1% (v/v) for 4 days. Cell viability was determined by measurement of luminescence monochromator, Synergy H4 Hybrid Reader (Bio Tek, Japan). The 50% inhibitory concentration (IC_{50}) and cell growth inhibitory concentration (GI_{50}) was determined by analyzing the log of the concentration-response curves by nonlinear regression analysis using the data analysis software, Origin (OriginLab, Northampton MA, US).

COLO-320DM and RKO cell growth inhibition MTT assay. To evaluate cell viability, Thiazolyl Blue Tetrazolium Bromide (MTT) (Sigma-Aldrich; M2128) was added at a final concentration of 1 mg/mL to cells treated with compounds for 5 days. These cells were incubated at 37 °C for 4 hours. Then the medium containing MTT was removed and dimethyl sulfoxide (DMSO) was added to the cells, following that optical density at 570 nm and 630 nm for reference were measured using xMark microplate spectrophotometer (Bio-RAD, Japan).

Western blot analysis (quantitation of AXIN2 accumulation). Cells treated with 0.33 μM or 0.1 μM compounds for 16 hours were harvested with lysis buffer (1% Nonidet-40, 150 mM NaCl, 50 mM Tris-HCl, pH 8.0) with 0.125 mM dithiothreitol, 2% (v/v) of protease inhibitor cocktail (Nacalai Tesque). Western blot analysis was performed as described previously.[42] The

primary antibodies were anti-Axin2 (76G6; 1:500; Cell Signaling Technology) and anti-GAPDH (6C5; 1:10000; Fitzgerald). Control samples (lysates of COLO-320DM treated with DMSO and G007-LK) were used for adjustment among the gels. Intensities of specific bands were quantified with ImageJ (NIH). The number of pixels of Axin2 bands was divided by that of GAPDH bands, then, the numeric value of the control samples treated with DMSO was considered as 1. All samples were normalized to the positive control samples treated with G007-LK.

Quantitative reverse transcription-polymerase chain reaction (qRT-PCR). Total RNAs were prepared with RNA basic kit (NIPPON Genetics, Tokyo, Japan) and cDNA were synthesized with RT Revertra Ace qPCR RT Master Mix (TOYOBO, Osaka, Japan). The expression levels of AXIN2, TCF7, AMOTL2, CTGF, and CYR61 mRNA were quantified by real-time PCR analysis with the LightCycler 480 Real-Time PCR System with Universal ProbeLibrary Probe #36, #3, #24, #85 and #66 (Roche, Indianapolis, IN, USA), respectively. ACTB mRNA was quantified using Universal ProbeLibrary Human ACTB Gene Assay (Roche, 05046165001) for normalization. The primers used were as follows: AXIN2, 5′-CACACCCTTCTCCAATCCAA-3′ (forward) and 5′-TGCCAGTTTCTTTGGCTCTT-3′ (reverse); TCF7, 5′-CCCACACTGTGAGCTGGTT-3′ (forward) and 5′-CAGCTCCTGCTTCCCTGA-3′ (reverse); AMOTL2, 5′-AGGCTGCAGAGAGACAATGAG-3′ (forward) and 5′-CTCAGAGAGCCGCTGGATT-3′ (reverse); CTGF, 5′-CTCCTGCAGGCTAGAGAAGC-3′ (forward) and 5′-GATGCACTTTTTGCCCTTCTT-3′ (reverse); and CYR61, 5′-

AAGAAACCCGGATTTGTGAG-3′ (forward) and 5′ -GCTGCATTTCTTGCCCTTT-3′ (reverse). The Tukey-Kramer test of R program was used for multiple comparisons of data.

Computational Methods

We used the X-ray structure of Tankyrase-2 and Compound **15d** (PDB ID: 6A84). For estimation effects of the introduction of halogen atom(s), we modified compound **15d** to **15**, **15a**, **15b**, **15c** in the X-ray structure. Modified atoms were minimized via AMBER10 EHT force field implemented in MOE[46]. All crystallization waters were removed. In this work, all of the FMO calculations were performed at the FMO2-MP2/6-31G* level using the ABINIT-MP program[47, 48]. Pair interaction energy decomposition analysis (PIEDA)[49, 50] was used to analyze the following energy components of inter-fragment interaction energy (IFIE; ΔE_{IJ}): electrostatic (ES), exchange-repulsion (EX), dispersion interaction (DI), and charge transfer with higher-order mixed terms (CT+mix) energies:

$$\Delta\tilde{\boldsymbol{E}}_{\boldsymbol{IJ}} = \Delta\tilde{\boldsymbol{E}}_{\mathbf{ES}} + \Delta\tilde{\boldsymbol{E}}_{\mathbf{EX}} + \Delta\tilde{\boldsymbol{E}}_{\mathbf{CT+mix}} + \Delta\tilde{\boldsymbol{E}}_{\mathbf{DI}}$$

Each protein–ligand system was divided into 212 fragments consisting of a compound and amino acids. A carbonyl group at main chain (X) is assigned to the subsequent fragment (X+1) because proteins are divided into fragments at localized orbitals (sp^3) between C_α and the carbon of carbonyl group in the FMO method.

Crystal structure determination

Tankyrase-2 protein preparation for crystallization. The PARP catalytic domain of human TNKS2 (residues 946–1162), containing an N-terminal modified natural poly-histidine affinity tag (N11; MKDHLIHNHHKHEHAHAEH), a FLAG tag, and a tobacco etch virus (TEV) protease cleavage site, was synthesized using the Escherichia coli cell-free protein synthesis system.[51, 52] The synthesized TNKS2 was first purified by a HisTrap HP column (GE Healthcare

Biosciences), and then cleaved by chymotrypsin (100:1 w/w). The two fragments (residues 947–1113 and residues 947–1162) generated by the cleavage were further purified by size-exclusion column chromatography with a HiLoad 16/60 Superdex 200 column (GE Healthcare Biosciences) equilibrated in 30 mM HEPES buffer (pH 7.5) containing 500 mM sodium chloride, 10% glycerol, and 500 μM TCEP.

Crystallization method. Crystals of human TNKS2 were obtained by the sitting drop method at 277 K. The reservoir solution for the complex with **1a** contained 100 mM Bis-Tris buffer (pH 6.5), 2% polyethylene glycol monomethyl ether 550, and 1.8 M ammonium sulphate. The reservoir solution for the complexes with **12**, **15d**, **52** and **40c** contained 100 mM Tris-HCl buffer (pH 8.5) and 2.4–2.5 M diammonium hydrogen phosphate. Crystals were soaked into the reservoir solution containing 1–3 mM inhibitor for four to five days. Soaked crystals were flash-cooled in liquid nitrogen using 20% glycerol as the cryoprotectant. Diffraction data were collected at the BL41XU and BL26B2 beamlines of Spring-8 (Harima, Japan) and at the AR-NE3A beamline of Photon Factory (Tsukuba, Japan) for the complexes with **1a**, **12**, **52**, and **40c** as listed in Supporting Information Table S10. They were processed with XDS[53] and the CCP4 suite[54]. Diffraction data for the complex with **15d** were collected in house using the Rigaku FR-X X-ray generator with a copper target, and were processed with HKL2000.[55] Molecular replacement was performed with Phaser[56] using the apo form of TNKS2 (PDB ID: 3KR7)[17]. The topology and parameter files for the inhibitors were generated with eLBOW[57] from SMILES strings. Structure refinement was performed using PHENIX[58] with manual model building using COOT[59]. Due to the protease treatment, the catalytic domain of TNKS2 is composed of two chains, for which separate chain IDs have been designated; chain A (residues 952-1113) and chain B (residues 1115-1162, or in the case of **40c**-bound TNKS2, residues 1116-1162).

Crystallographic statistics are summarized in Supporting Information Table S10. The coordinates and structure factors have been deposited at the Protein Data Bank with the accession codes 5ZQO, 6A84, 5ZQP, 5ZQQ **a**nd 5ZQR for the complexes with **1a**, **15d**, **12**, **52** and **40c**, respectively.

■ ASOCIATED CONTENT

The Supporting Information is available free of charge on the ACS Publications website at http://pubs.acs.org.

Additional figures illustrating data for HTS, fragment-orbital method, X-ray crystallography, biological assay, and analytical data for final compounds (pdf)

Molecular formula strings and some data (csv)

Accession Codes Coordinates and structure factors have been deposited at the Protein Data Bank with codes 5ZQO, 6A84, 5ZQP, 5ZQQ and 5ZQR.

■ AUTHOR INFORMATION

Corresponding Author

*F.Shirai: phone, +81484678792; e-mail, fumiyuki.shirai@riken.jp.

*H.Koyama: phone, +81484679253; e-mail, hiroo.koyama@riken.jp.

■ ACKNOWLEDGEMENTS

We thank Fumiko Kyotani, Satsuki Irie for their efforts in evaluating compounds in aqueous solubility, PAMPA and microsomal stability experiments, Mika Takagi for *in vitro* enzyme and cell assay, Dr. Takemichi Nakamura for his assistance in high-resolution mass spectrometry and Mie Goto, Mio Inoue, Ken Ishii, and Toshi Arima for protein samples preparation. We thank Dr. Kenji Mori for helpful discussion. FMO study was performed in the framework of the FMO drug design consortium (FMODD). This research was supported by RIKEN Program for Drug

Discovery and Medical Technology Platforms and Japan Agency for Medical Research and Development (AMED) under Grant Numbers JP17am0101086, 15cm0106004 (to M.Y.), JP15cm0106030 (to HS and YY) and JP16cm0106102, JP17cm0106102, JP18cm0106102 (to HS and YY).

■ ABBREVIATIONS USED

APC, adenomatous polyposis coli; AXIN, axis inhibition protein; AUC, Area Under the Curve; BID, twice daily; CRC, colorectal cancer; C_{max}, maximum concentration; DMPK, Drug metabolism and pharmacokinetics; MDCK II, Madin-Darby canine kidney cell II; ELISA, enzyme-linked immunosorbent assay; PARP, poly(ADP-ribose) polymerase; PARsylation, poly-ADP-ribosylation; P-gp, P-glycoprotein; THQ, tetrahydroquinazolinone; TGI, Tumor growth inhibition; TNKS, telomere-associated poly(ADP-ribose) polymerase tankyrase; HTS, High-throughput screening; DIPEA; Diisopropylethylamine; p-TsOH, *p*-Toluenesulfonic acid.

■ REFERENCES

1. Pinto, D.; Clevers, H. Wnt control of stem cells and differentiation in the intestinal epithelium. *Exp. Cell Res.* **2005,** *306*, 357-363.
2. Lu, B.; Green, B. A.; Farr, J. M.; Lopes, F. C.; Van Raay, T. J. Wnt drug discovery: Weaving through the screens, patents and clinical trials. *Cancers (Basel)* **2016,** 8.
3. Segditsas, S.; Tomlinson, I. Colorectal cancer and genetic alterations in the Wnt pathway. *Oncogene* **2006,** *25*, 7531-7537.
4. Reya, T.; Clevers, H. Wnt signalling in stem cells and cancer. *Nature* **2005,** *434*, 843-850.
5. Markowitz, S. D.; Bertagnolli, M. M. Molecular origins of cancer: Molecular basis of colorectal cancer. *New Engl. J. Med.* **2009,** *361*, 2449-2460.
6. Lui, T. T.; Lacroix, C.; Ahmed, S. M.; Goldenberg, S. J.; Leach, C. A.; Daulat, A. M.; Angers, S. The ubiquitin-specific protease USP34 regulates axin stability and Wnt/β-catenin signaling. *Mol. Cell Biol.* **2011,** *31*, 2053-2065.
7. Masuda, M.; Sawa, M.; Yamada, T. Therapeutic targets in the Wnt signaling pathway: feasibility of targeting TNIK in colorectal cancer. *Pharmacol. Ther.* **2015,** *156*, 1-9.
8. Voronkov, A.; Krauss, S. Wnt/beta-catenin signaling and small molecule inhibitors. *Curr. Pharm. Des.* **2013,** *19*, 634-664.
9. Schreiber, V.; Dantzer, F.; Ame, J. C.; de Murcia, G. Poly (ADP-ribose): Novel functions for an old molecule. *Nat. Rev. Mol. Cell Biol.* **2006,** *7*, 517-528.
10. Huang, S. M.; Mishina, Y. M.; Liu, S.; Cheung, A.; Stegmeier, F.; Michaud, G. A.; Charlat, O.; Wiellette, E.; Zhang, Y.; Wiessner, S.; Hild, M.; Shi, X.; Wilson, C. J.; Mickanin, C.; Myer, V.; Fazal, A.; Tomlinson, R.; Serluca, F.; Shao, W.; Cheng, H.; Shultz, M.; Rau, C.; Schirle, M.; Schlegl, J.; Ghidelli, S.; Fawell, S.; Lu, C.; Curtis, D.; Kirschner, M. W.;

Lengauer, C.; Finan, P. M.; Tallarico, J. A.; Bouwmeester, T.; Porter, J. A.; Bauer, A.; Cong, F. Tankyrase inhibition stabilizes axin and antagonizes Wnt signalling. *Nature* **2009,** *461*, 614-620.

11. Leung J.Y.; Kolligs F.T.; Wu R.; Zhai Y.; Kuick R.; Hanash S.; Cho K.R.; Fearon E.R. Activation of AXIN2 expression by beta-catenin-T cell factor. A feedback repressor pathway regulating Wnt signaling. *J. Biol. Chem.* **2002,** *277*, 21657-21665.
12. Smith S.; de Lange T. Tankyrase promotes telomere elongation in human cells. *Curr. Biol.* **2000,** *10*, 1299-1302.
13. Wang W.; Li N.; Li X.; Tran M.K.; Han X.; Chen J. Tankyrase inhibitors target YAP by stabilizing angiomotin family proteins. *Cell Rep.* **2015,** *13*, 524-532.
14. Smith S.; de Lange T. Cell cycle dependent localization of the telomeric PARP, tankyrase, to nuclear pore complexes and centrosomes. *J. Cell Sci.* **1999,** *112*, 3649-3656.
15. Chi N.W.; Lodish H.F. Tankyrase is a golgi-associated mitogen-activated protein kinase substrate that interacts with IRAP in GLUT4 vesicles. *J. Biol. Chem.* 2000, *275*, 38437-38444.
16. Thorvaldsen, T. E. Targeting tankyrase to fight WNT-dependent tumors. *Basic Clin. Pharmacol. Toxicol.* **2017,** *121*, 81-88.
17. Karlberg, T.; Markova, N.; Johansson, I.; Hammarström, M.; Schütz, P.; Weigelt, J.; Schüler, H. Structural basis for the interaction between tankyrase-2 and a potent Wnt-signaling inhibitor. *J. Med. Chem.* **2010,** *53*, 5352-5355.
18. Waaler, J.; Machon, O.; von Kries, J. P.; Wilson, S. R.; Lundenes, E.; Wedlich, D.; Gradl, D.; Paulsen, J. E.; Machonova, O.; Dembinski, J. L.; Dinh, H.; Krauss, S. Novel synthetic

antagonists of canonical Wnt signaling inhibit colorectal cancer cell growth. *Cancer Res.* **2011,** *71*, 197-205.

19. Waaler, J.; Machon, O.; Tumova, L.; Dinh, H.; Korinek, V.; Wilson, S. R.; Paulsen, J. E.; Pedersen, N. M.; Eide, T. J.; Machonova, O.; Gradl, D.; Voronkov, A.; von Kries, J. P.; Krauss, S. A novel tankyrase inhibitor decreases canonical Wnt signaling in colon carcinoma cells and reduces tumor growth in conditional APC mutant mice. *Cancer Res.* **2012,** *72*, 2822-2832.
20. Voronkov, A.; Holsworth, D. D.; Waaler, J.; Wilson, S. R.; Ekblad, B.; Perdreau-Dahl, H.; Dinh, H.; Drewes, G.; Hopf, C.; Morth, J. P.; Krauss, S. Structural basis and SAR for G007-LK, a lead stage 1,2,4-triazole based specific tankyrase 1/2 inhibitor. *J. Med. Chem.* **2013,** *56*, 3012-3023.
21. Lau, T.; Chan, E.; Callow, M.; Waaler, J.; Boggs, J.; Blake, R. A.; Magnuson, S.; Sambrone, A.; Schutten, M.; Firestein, R.; Machon, O.; Korinek, V.; Choo, E.; Diaz, D.; Merchant, M.; Polakis, P.; Holsworth, D. D.; Krauss, S.; Costa, M. A novel tankyrase small-molecule inhibitor suppresses APC mutation-driven colorectal tumor growth. *Cancer Res.* **2013,** *73*, 3132-3144.
22. Shultz, M. D.; Cheung, A. K.; Kirby, C. A.; Firestone, B.; Fan, J.; Chen, C. H.; Chen, Z.; Chin, D. N.; Dipietro, L.; Fazal, A.; Feng, Y.; Fortin, P. D.; Gould, T.; Lagu, B.; Lei, H.; Lenoir, F.; Majumdar, D.; Ochala, E.; Palermo, M. G.; Pham, L.; Pu, M.; Smith, T.; Stams, T.; Tomlinson, R. C.; Touré, B. B.; Visser, M.; Wang, R. M.; Waters, N. J.; Shao, W. Identification of NVP-TNKS656: The use of structure-efficiency relationships to generate a highly potent, selective, and orally active tankyrase inhibitor. *J. Med. Chem.* **2013,** *56*, 6495-6511.

23. Arqués, O.; Chicote, I.; Puig, I.; Tenbaum, S. P.; Argilés, G.; Dienstmann, R.; Fernández, N.; Caratù, G.; Matito, J.; Silberschmidt, D.; Rodon, J.; Landolfi, S.; Prat, A.; Espín, E.; Charco, R.; Nuciforo, P.; Vivancos, A.; Shao, W.; Tabernero, J.; Palmer, H. G. Tankyrase inhibition blocks Wnt/β-catenin pathway and reverts resistance to PI3K and AKT inhibitors in the treatment of colorectal cancer. *Clin. Cancer Res.* **2016,** *22*, 644-656.

24. Johannes, J. W.; Almeida, L.; Barlaam, B.; Boriack-Sjodin, P. A.; Casella, R.; Croft, R. A.; Dishington, A. P.; Gingipalli, L.; Gu, C.; Hawkins, J. L.; Holmes, J. L.; Howard, T.; Huang, J.; Ioannidis, S.; Kazmirski, S.; Lamb, M. L.; McGuire, T. M.; Moore, J. E.; Ogg, D.; Patel, A.; Pike, K. G.; Pontz, T.; Robb, G. R.; Su, N.; Wang, H.; Wu, X.; Zhang, H. J.; Zhang, Y.; Zheng, X.; Wang, T. Pyrimidinone nicotinamide mimetics as selective tankyrase and wnt pathway inhibitors suitable for in vivo pharmacology. *ACS Med. Chem. Lett.* **2015,** *6*, 254-259.

25. Quackenbush, K. S.; Bagby, S.; Tai, W. M.; Messersmith, W. A.; Schreiber, A.; Greene, J.; Kim, J.; Wang, G.; Purkey, A.; Pitts, T. M.; Nguyen, A.; Gao, D.; Blatchford, P.; Capasso, A.; Schuller, A. G.; Eckhardt, S. G.; Arcaroli, J. J. The novel tankyrase inhibitor (AZ1366) enhances irinotecan activity in tumors that exhibit elevated tankyrase and irinotecan resistance. *Oncotarget* **2016,** *7*, 28273-28785.

26. McGonigle, S.; Chen, Z.; Wu, J.; Chang, P.; Kolber-Simonds, D.; Ackermann, K.; Twine, N. C.; Shie, J. L.; Miu, J. T.; Huang, K. C.; Moniz, G. A.; Nomoto, K. E7449: A dual inhibitor of PARP1/2 and tankyrase1/2 inhibits growth of DNA repair deficient tumors and antagonizes Wnt signaling. *Oncotarget* **2015,** *6*, 41307-41323.

27. Zhong, Y.; Katavolos, P.; Nguyen, T.; Lau, T.; Boggs, J.; Sambrone, A.; Kan, D.; Merchant, M.; Harstad, E.; Diaz, D.; Costa, M.; Schutten, M. Tankyrase inhibition causes reversible intestinal toxicity in mice with a therapeutic index < 1. *Toxicol. Pathol.* **2016,** *44*, 267-278.

28. Mariotti, L.; Pollock, K.; Guettler, S. Regulation of Wnt/β-catenin signalling by tankyrase-dependent poly(ADP-ribosyl)ation and scaffolding. *Br. J. Pharmacol.* **2017,** *174*, 4611-4636.

29. Scarborough, H. A.; Helfrich, B. A.; Casás-Selves, M.; Schuller, A. G.; Grosskurth, S. E.; Kim, J.; Tan, A. C.; Chan, D. C.; Zhang, Z.; Zaberezhnyy, V.; Bunn, P. A.; DeGregori, J. AZ1366: An inhibitor of tankyrase and the canonical Wnt pathway that limits the persistence of non-small cell lung cancer cells following EGFR inhibition. *Clin. Cancer Res.* **2017,** *23*, 1531-1541.

30. Dziaman, T.; Ludwiczak, H.; Ciesla, J. M.; Banaszkiewicz, Z.; Winczura, A.; Chmielarczyk, M.; Wisniewska, E.; Marszalek, A.; Tudek, B.; Olinski, R. PARP-1 expression is increased in colon adenoma and carcinoma and correlates with OGG1. *PLoS One* **2014,** *9*, e115558.

31. Gupta C.M.; Bhaduri A.P.; Khanna N.M.; Mukherjee Surath K. Novel class of hypoglycemic agents: syntheses and SAR [sodium absorption ratio] in 2-substituted 4(3*H*)-quinazolones, 2-substituted 4-hydroxypolymethylene [5,6] pyrimidines, and 3-substituted 4-oxopyrido [1,2-*a*] pyrimidines. *Indian J. Chem.* **1971,** *9*, 201-206.

32. Masuda, T.; Tachibana Y.; Miyagawa, M.; Hasegawa, T.; Tobinaga H. Pyrimidine Derivatives and Pharmaceutical Composition Containing Same. WO 2011/078,143 A1, Jun 30, 2011.

33. Buchstaller, H-P.; Esdar, C.; Leuthner, B. Tetrahydoquinazolinone Derivatives as TANK and PARP Inhibitors. WO 2013/117,288 A1, Aug 15, 2013.

34. Kitaura, K.; Ikeo, E.; Asada, T.; Nakano, T.; Uebayasi, M. Fragment molecular orbital method: An approximate computational method for large molecules. *Chem. Phys. Lett.* **1999,** *313*, 701-706.

35. Fedorov, D. G.; Kitaura, K. The Fragment Molecular Orbital Method: Practical Applications to Large Molecular Systems; CRC Press: Boca Raton, FL, 2009.

36. Tanaka, S.; Mochizuki, Y.; Komeiji, Y.; Okiyama, Y.; Fukuzawa, K. Electron-correlated fragment-molecular-orbital calculations for biomolecular and nano systems. *Phys. Chem. Chem. Phys.* **2014,** *16*, 10310-10344.

37. Guidance for Industry Drug Interaction Studies - Study Design, Data Analysis, Implications for Dosing, and Labeling Recommendations; U.S. Department of Health and Human Services Food and Drug Administration Center for Drug Evaluation and Research (CDER): Silver Spring, MD, February 2012.

38. Mistry, P.; Stewart, A. J.; Dangerfield, W.; Okiji, S.; Liddle, C.; Bootle, D.; Plumb, J. A.; Templeton, D.; Charlton, P. In vitro and in vivo reversal of P-glycoprotein-mediated multidrug resistance by a novel potent modulator, XR9576. *Cancer Res.* **2001,** *61*, 749-758.

39. Callaghan, R.; Luk, F.; Bebawy, M. Inhibition of the multidrug resistance P-glycoprotein: Time for a change of strategy? *Drug Metab. Dispos.* **2014,** *42*, 623-631.

40. Thorsell A-G.; Ekblad T.; Karlberg T.; Löw M.; Pinto A.F.; Trésaugues L.; Moche M.; Cohen M.S.; Schüler H. Structural basis for potency and promiscuity in poly(ADP-ribose) polymerase (PARP) and tankyrase inhibitors. *J. Med. Chem.* **2017,** *60*, 1262-1271.

41. Jia J.; Qiao Y.; Pilo M.G.; Cigliano A.; Liu X.; Shao Z.; Calvisi D.F.; Chen X.; Tankyrase inhibitors suppress hepatocellular carcinoma cell growth via modulating the Hippo cascade. *PLoS One.* **2017,** *12*, e0184068.

42. Mizutani, A.; Yashiroda, Y.; Muramatsu, Y.; Yoshida, H.; Chikada, T.; Tsumura, T.; Okue, M.; Shirai, F.; Fukami, T.; Yoshida, M.; Seimiya, H. RK-287107, a potent and specific tankyrase inhibitor, blocks colorectal cancer cell growth in a preclinical model. *Cancer Sci.* **2018**, *109*, 4003-4014.

43. Anumala U.R.; Waaler J.; Nkizinkiko Y.; Ignatev A.; Lazarow K.; Lindemann P.; Olsen P.A.; Murthy S.; Obaji E.; Majouga A.G.; Leonov S.; von Kries J.P.; Lehtiö L.; Krauss S.; Nazaré M. Discovery of a novel series of tankyrase inhibitors by a hybridization approach. *J. Med. Chem.* **2017,** *60*, 10013-10025.

44. Yashiroda, Y.; Okamoto, R.; Hatsugai, K.; Takemoto, Y.; Goshima, N.; Saito, T.; Hamamoto, M.; Sugimoto, Y.; Osada, H.; Seimiya, H.; Yoshida, M. A novel yeast cell-based screen identifies flavone as a tankyrase inhibitor. *Biochem. Biophys. Res. Commun.* **2010**, *394*, 569-573.

45. Fonsi, M.; Orsale, M.V.; Monteagudo, E. High-throughput microsomal stability assay for screening new chemical entities in drug discovery. *J. Biomol. Screen* **2008**, *13*, 862-869.

46. Molecular Operating Environment (MOE 2018.0101); Chemical Computing Group: Montreal, QC, Canada, 2018.

47. Nakano T.; Kaminuma T.; Sato T.; Akiyama Y.; Uebayasi M.; Kitaura K. Fragment molecular orbital method: application to polypeptides. *Chem. Phys. Lett.* **2000,** *318*, 614-618.

48. MIZUHO/BioStation Viewer 3.0, Mizuho information and research institute Inc., Tokyo, Japan, 2013.

49. Fedorov, D. G.; Kitaura, K. Pair interaction energy decomposition analysis. *J. Comp. Chem.* **2007,** *28*, 222-237.

50. Tsukamoto, T.; Kato, K.; Kato, A.; Nakano, T.; Mochizuki, Y.; Fukuzawa, K. Implementation of pair interaction energy decomposition analysis and its applications to protein-ligand systems. *J. Comput. Chem. Jpn.* **2015,** *14*, 1-9.

51. Terada, T.; Murata, T.; Shirouzu, M.; Yokoyama, S. Cell-free expression of protein complexes for structural biology. *Methods Mol. Biol.* **2014**, *1091*, 151-159.

52. Katsura, K.; Matsuda, T.; Tomabechi, Y.; Yonemochi, M.; Hanada, K; Ohsawa, N.; Sakamoto, K.; Takemoto, C.; Shirouzu, M. A reproducible and scalable procedure for preparing bacterial extracts for cell-free protein synthesis. *J. Biochem.* **2017**, *162*, 357-369.

53. Kabsch, W. XDS. *Acta Crystallogr. D Biol. Crystallogr.* **2010,** *66*, 125-132.

54. Winn, M. D.; Ballard, C. C.; Cowtan, K. D.; Dodson, E. J.; Emsley, P.; Evans, P. R.; Keegan, R. M.; Krissinel, E. B.; Leslie, A. G.; McCoy, A.; McNicholas, S. J.; Murshudov, G. N.; Pannu, N. S.; Potterton, E. A.; Powell, H. R.; Read, R. J.; Vagin, A.; Wilson, K. S. Overview of the CCP4 suite and current developments. *Acta Crystallogr., Sect. D: Biol. Crystallogr.* **2011,** *67*, 235-242.

55. Otwinowski, Z.; Minor, W. Processing of X-ray diffraction data collected in oscillation mode. *Methods Enzymol.* **1997,** *276*, 307-326.

56. McCoy, A. J.; Grosse-Kunstleve, R. W.; Adams, P. D.; Winn, M. D.; Storoni, L. C.; Read, R. J. Phaser crystallographic software. *J. Appl. Crystallogr.* **2007,** *40*, 658-674.

57. Moriarty, N. W.; Grosse-Kunstleve, R. W.; Adams, P. D. Electronic ligand builder and optimization workbench (eLBOW): A tool for ligand coordinate and restraint generation. *Acta Crystallogr., Sect. D: Biol. Crystallogr.* **2009,** *65*, 1074-1080.

58. Adams, P. D.; Afonine, P. V.; Bunkóczi, G.; Chen, V. B.; Davis, I. W.; Echols, N.; Headd, J. J.; Hung, L. W.; Kapral, G. J.; Grosse-Kunstleve, R. W.; McCoy, A. J.; Moriarty, N. W.;

Oeffner, R.; Read, R. J.; Richardson, D. C.; Richardson, J. S.; Terwilliger, T. C.; Zwart, P. H. PHENIX: A comprehensive Python-based system for macromolecular structure solution. *Acta Crystallogr., Sect. D: Biol. Crystallogr.* **2010,** *66*, 213-221.

59. Emsley, P.; Lohkamp, B.; Scott, W. G.; Cowtan, K. Features and development of Coot. *Acta Crystallogr., Sect. D: Biol. Crystallogr.* **2010,** *66*, 486-501.

Figure 1. Structure of selected tankyrase inhibitors that have been reported in the literature (tankyrase binding pocket is indicated in parentheses).

Figure 2. Structural development from the HTS hit compound **1a** to the lead compound supported by X-ray crystallography. Structural basis of choosing bicyclic spiro scaffold.

Figure 3. (A) Compound **1a** (green; PDB ID: 5ZQO) in the complex crystal structure is shown in green with stick representation. Blue and black dashed lines denote hydrogen bonds and π-π/CH-π interactions. The backbone is shown with a ribbon and the nook region in blue. (B) Side view of the bound compound.

Figure 4. Side view of bound compounds to emphasize spiro moiety. Compound **12** (magenta; PDB ID: 5ZQP) and **1a** (green; PDB ID: 5ZQO) in the complex crystal structures are shown as stick representations. Blue and black dashed lines denote hydrogen bonds and π-π/CH-π interactions, respectively.

Figure 5. Compound **40c** is shown in blue as a stick representation. Blue and black dashed lines denote hydrogen bonds and π–π/CH-π interactions, respectively (PDB ID: 5ZQR). The residues interacting in the same way as compound **1a** are shown in gray.

Figure 6. Pharmacokinetics (mouse intraperitoneal 50mg/kg injection) of the selected compounds (**40c**, **40d**, **43c** and **43d**). PK parameter of these compounds is presented at Table 6.

Shirai *et al.* Figure 1.

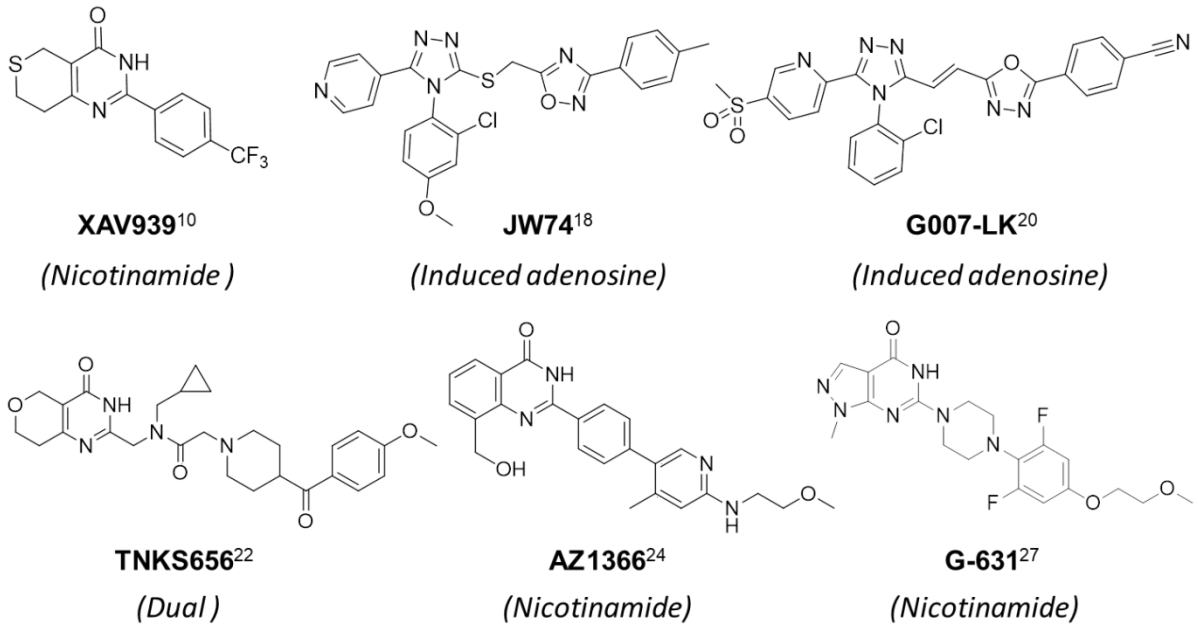

Shirai *et al.* Figure 2.

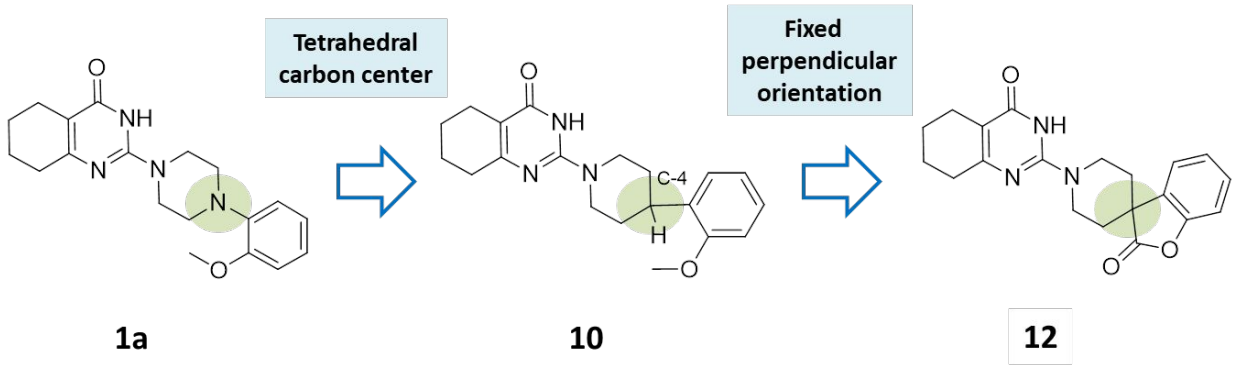

Shirai *et al.* Figure 3.

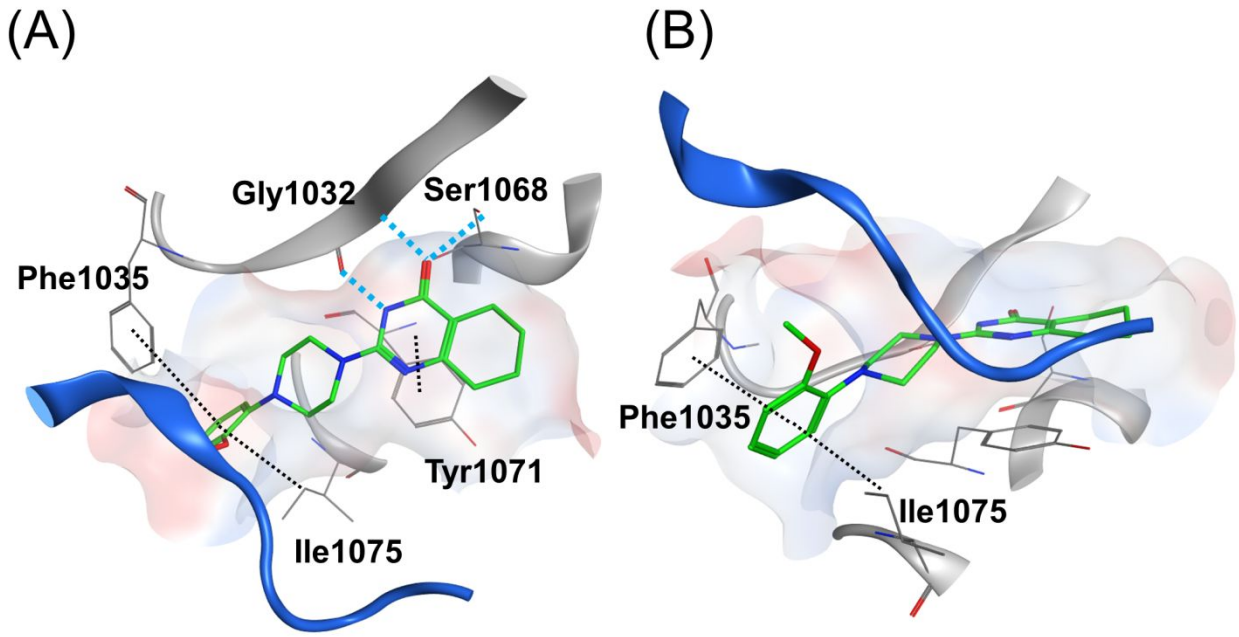

Shirai *et al.* Figure 4.

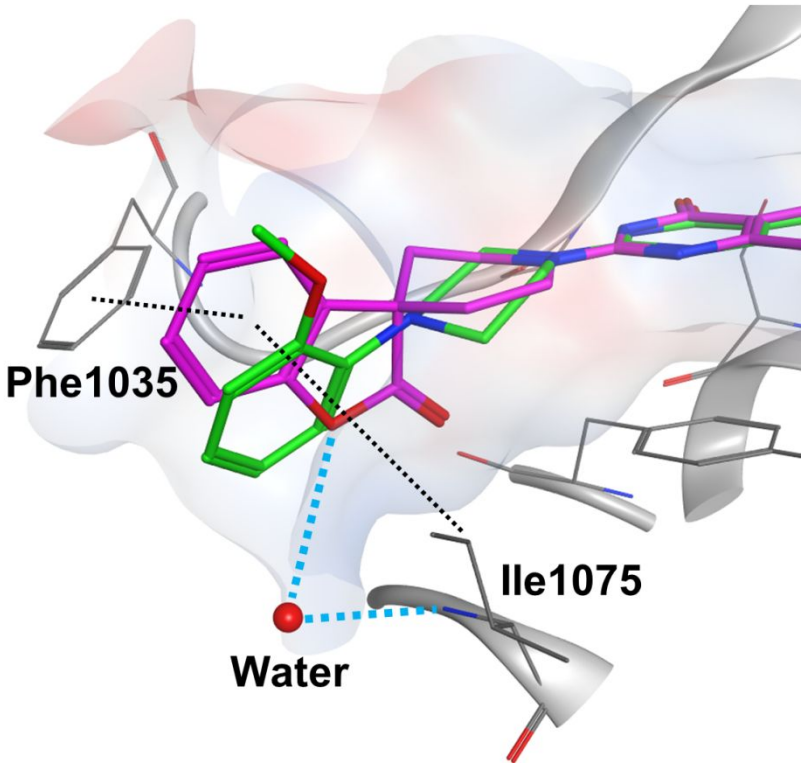
Phe1035
Ile1075
Water

Shirai *et al.* Figure 5.

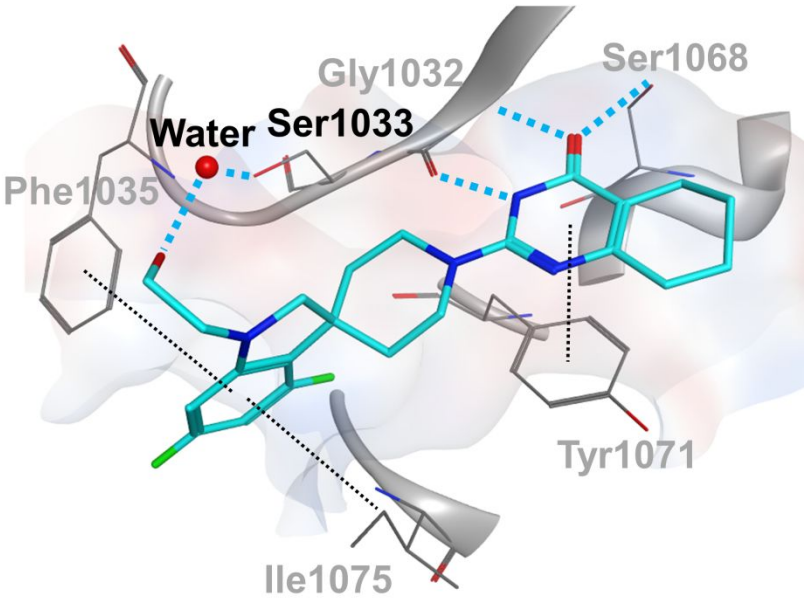

Shirai *et al.* Figure 6.

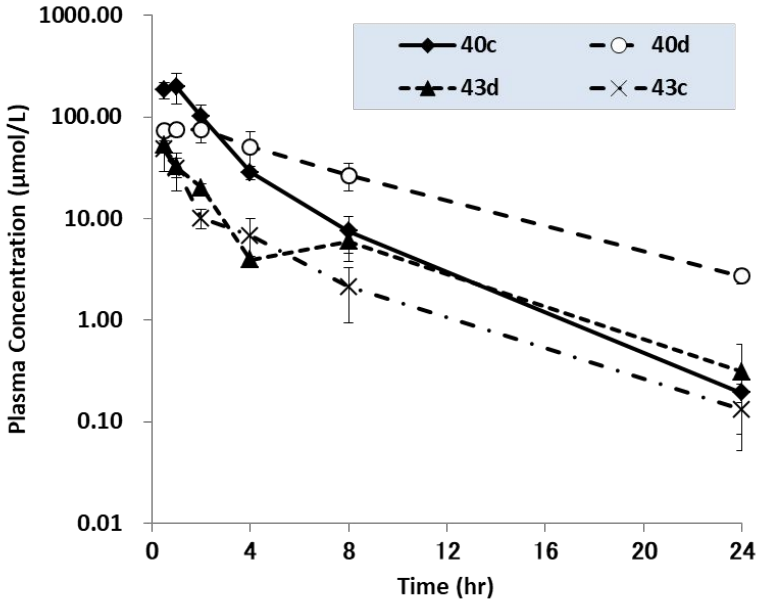

Scheme 1. Synthesis of **1a** analogues [a]

[a]Reagents and conditions: (a) **3c**, **3e**: Diethylcarbonate, t-BuOK, -10 °C; **3f**, **3h**: Diethylcarbonate, NaH, -10 °C; (b) t-BuOK, Toluene, rt; (c) *S*-methylisothiourea sulfate, K_2CO_3, water, rt; (d) Toluene, reflux; (e) (1) Toluene, reflux; (2) 4NHCl/dioxane, rt; (f) formaldehyde, $NaBH_3CN$, AcOH, MeOH, rt; (g) *m*-CPBA, DCM, rt.

Scheme 2. Synthesis of derivatives with various THQ–phenyl ring connecting structures [a]

[a]Reagents and conditions: (a) Toluene, reflux; (b) (1) *m*-CPBA, DCM, -17 °C; (2) Et_3N, DME, rt; (c) 1-amidinopyrazole hydrochloride, DIPEA, CH_3CN, rt; (d) **3a**, K_2CO_3, THF-water, 60 °C; (e) (1) NH_2OH HCl, KOH, MeOH, 90 °C; (2) H_2, Ac_2O, CH_3CO_2H.

Scheme 3. Synthesis of the substituted spiroindoline/indolinone derivatives [a]

[a]Reagents and conditions: (a) 1-amidinopyrazole hydrochloride, DIPEA, CH_3CN, rt; (b) **3a**, K_2CO_3, THF-water, 60 °C; (c) CF_3CO_2H, DCM, rt; (d) (1) CF_3CO_2H, $CHCl_3$, 35 °C; (2) $NaBH(OAc)_3$, rt ; (e) CF_3CO_2H, reflux; (f) (1) Boc_2O, imidazole, DCM, rt; (2) H_2, 10%Pd-Carbon, MeOH, rt, 1atm; (g) (1) CF_3CO_2H, $CHCl_3$, reflux; (2) *m*-CPBA, rt.

Scheme 4. Synthesis of the substituted 1-(2-hydroxyethyl)-spiroindoline/indolinone derivatives [a]

[a]Reagents and conditions: (a) Glycolaldehyde dimer, $NaBH(OAc)_3$, $CHCl_3$, rt; (b) (1) $ClCH_2CH_2OTHP$, NaH, NaI, DMF, 80 °C; (2) pTsOH; (c) CF_3CO_2H, reflux: (d) (1) 1-Amidinopyrazole hydrochloride, Et_3N, CH_3CN, rt; (2) **3a**, EtONa, EtOH, reflux; (e) 2-Chloro-5,6,7,8-tetrahydroquinazolin-4(3*H*)-one (**51**), Et_3N, EtOH, Microwave 120 °C; (f) $(ClCH_2CH_2)_2NBn$, NaH, DMF, 0–55 °C; (g) (1) 95% H_2SO_4, 80 °C; (2) LiH, NMP, 5–120 °C; (h) $LiAlH_4$, THF, reflux; (i) $BrCH_2CH_2OH$, THF, Microwave 130 °C; (j) 20% $Pd(OH)_2$-Carbon, H_2, EtOH, rt; (k) $BrCH_2CH_2OH$, K_2CO_3, DMF, 70 °C.

Shirai *et al.* Scheme 1.

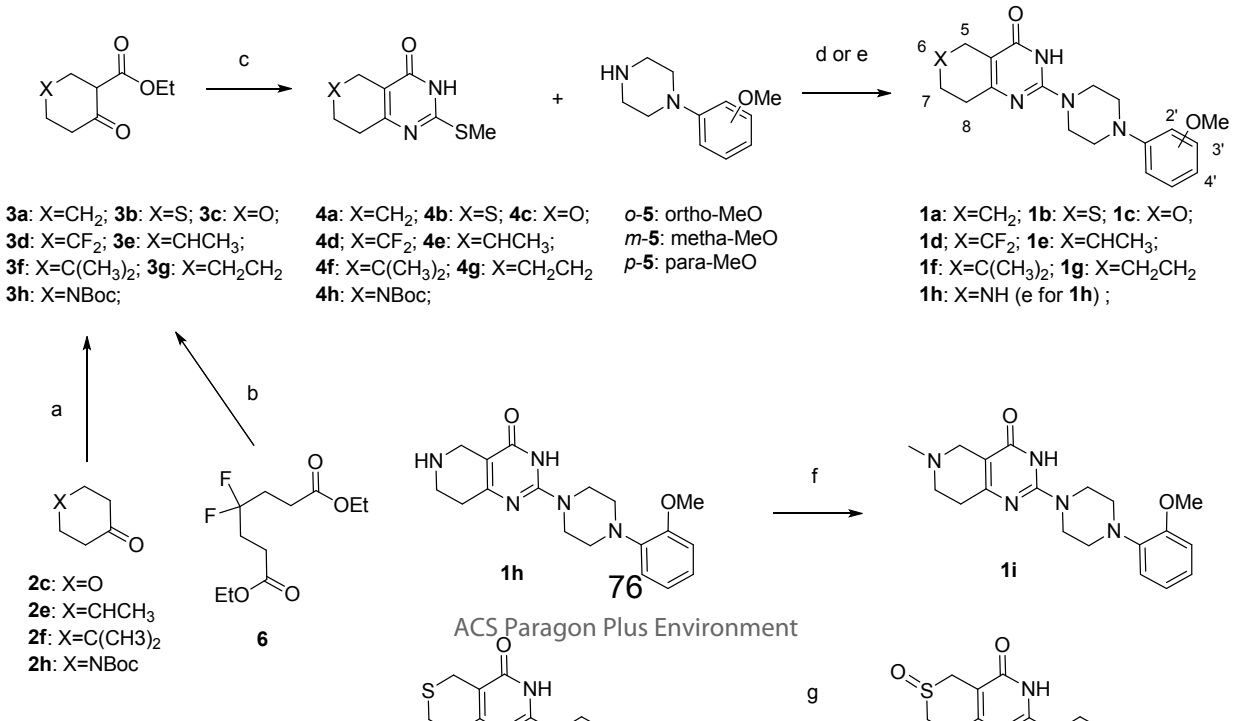

Shirai *et al.* Scheme 2.

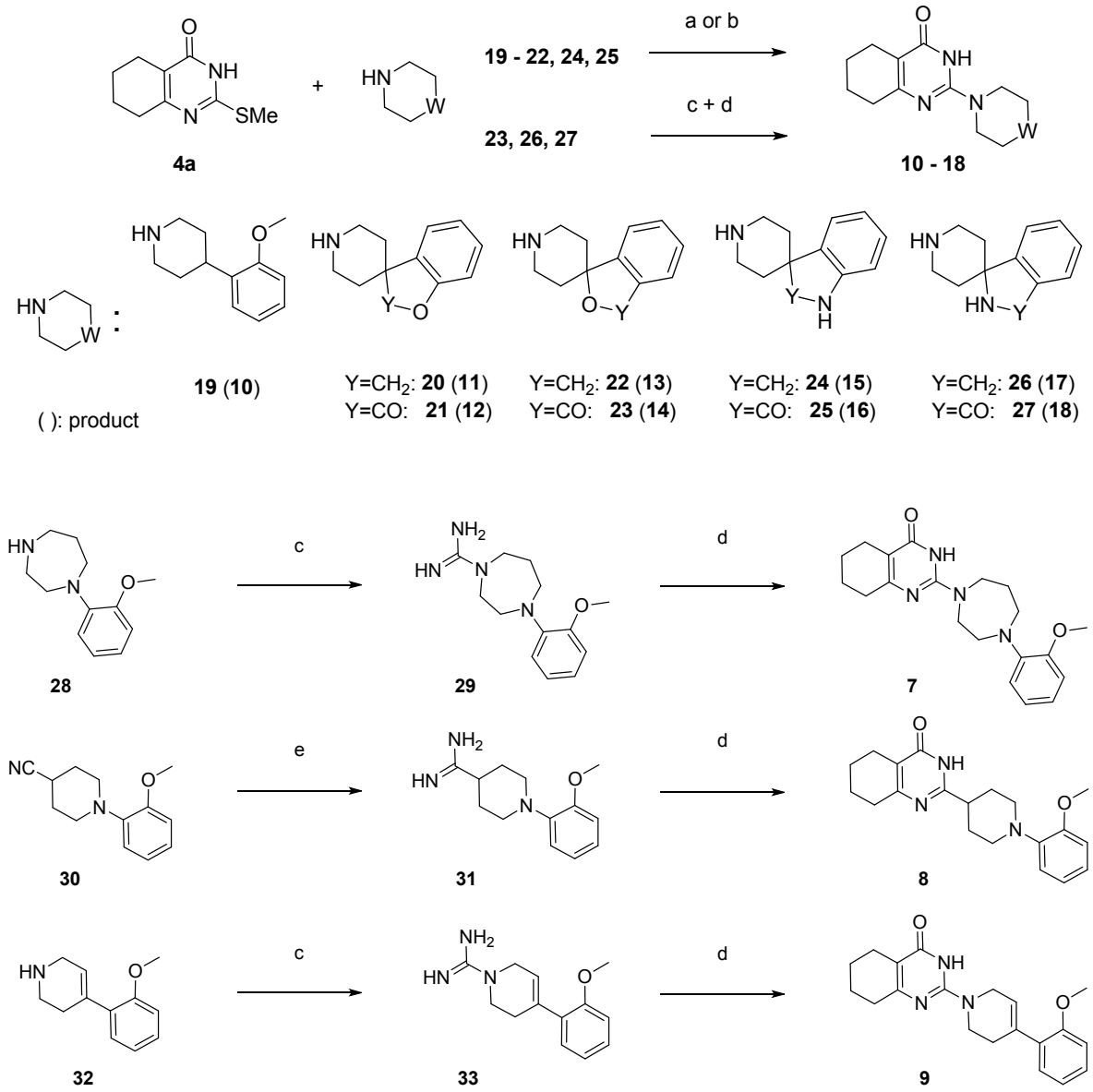

Shirai *et al.* Scheme 3.

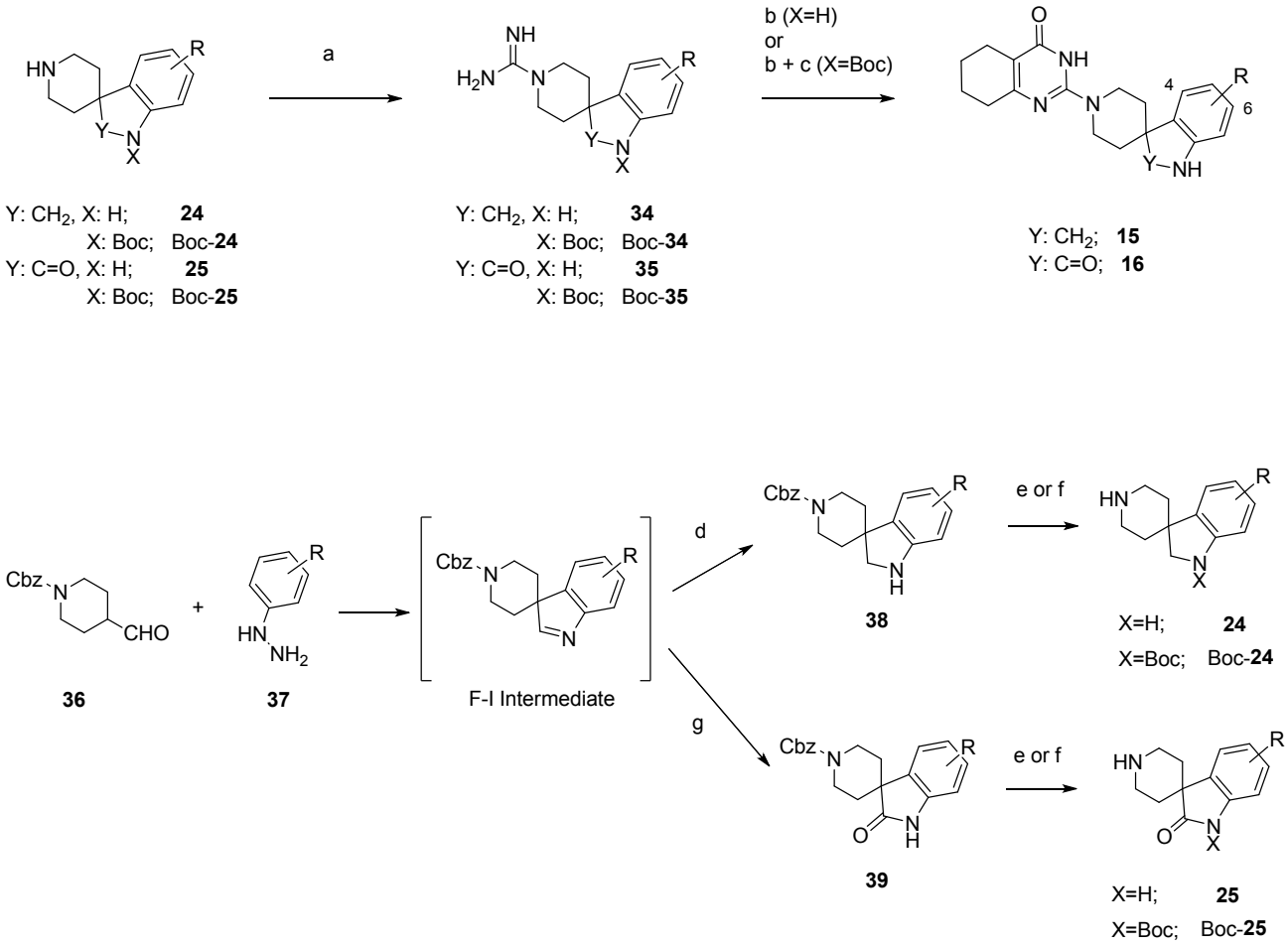

Shirai *et al.* Scheme 4.

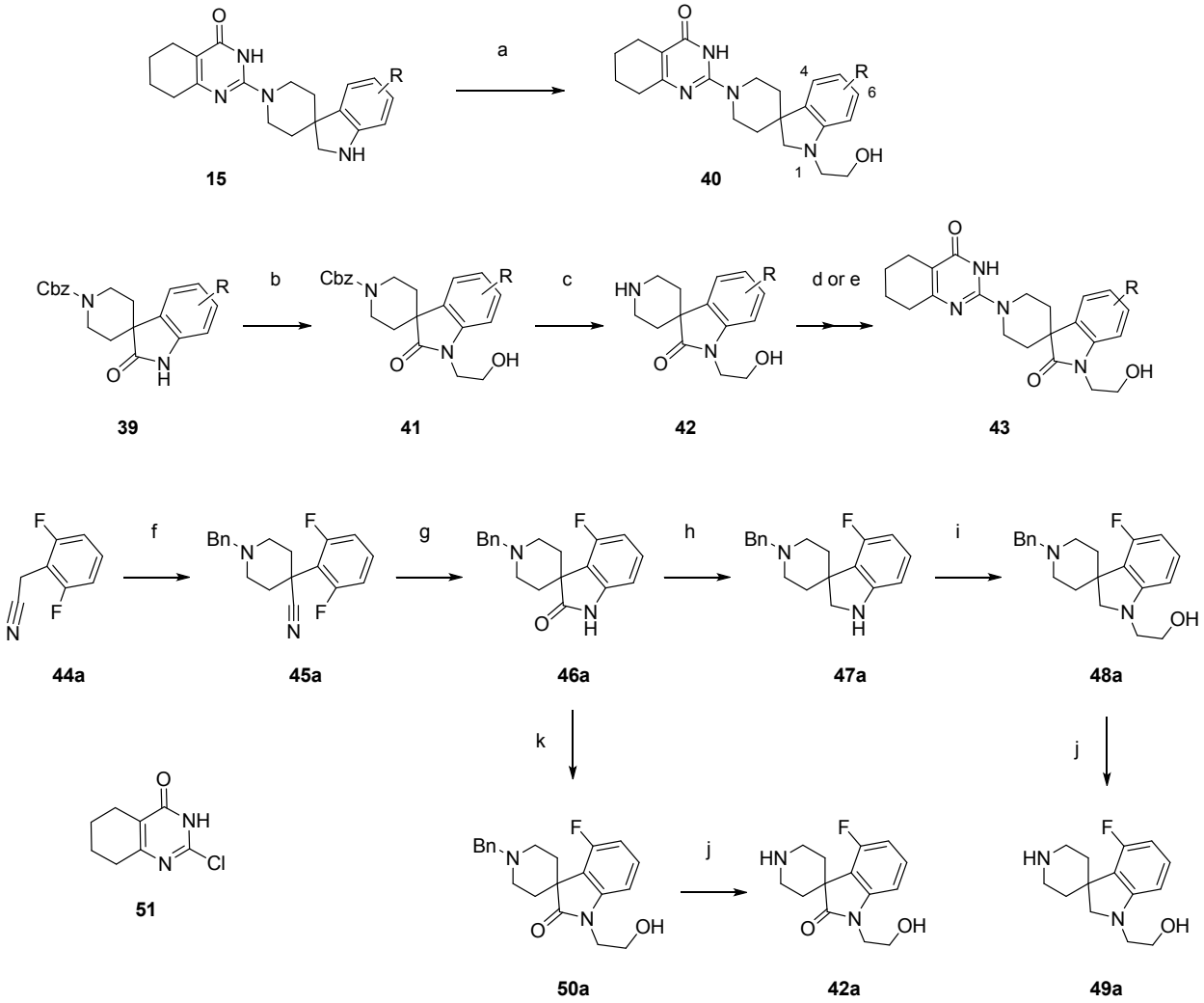

Shirai *et al.* Table of Contents graphic

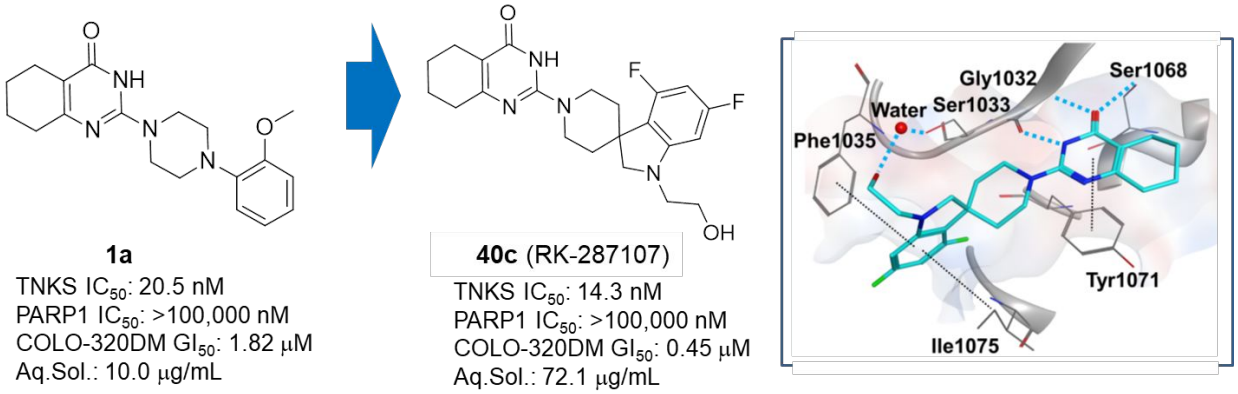

1a
TNKS IC_{50}: 20.5 nM
PARP1 IC_{50}: >100,000 nM
COLO-320DM GI_{50}: 1.82 μM
Aq.Sol.: 10.0 μg/mL

40c (RK-287107)
TNKS IC_{50}: 14.3 nM
PARP1 IC_{50}: >100,000 nM
COLO-320DM GI_{50}: 0.45 μM
Aq.Sol.: 72.1 μg/mL